DEVELOPING A DATASET FOR SIMULATING URBAN CLIMATE IMPACTS ON A GLOBAL SCALE

By

Trisha Jackson

Submitted to the graduate degree program in Geography
and the Faculty of the Graduate School of the University of Kansas
In partial fulfillment of the requirements for the degree of
Master's of Arts

____
Johannes J. Feddema, Chairperson

Committee members: ______________________________
William C. Johnson

____
Stephen L. Egbert

Date defended:____May 22, 2007_______

The Thesis Committee for Trisha Jackson certifies
That this is the approved version of the following thesis:

DEVELOPING A DATASET FOR SIMULATING
URBAN CLIMATE IMPACTS ON A GLOBAL SCALE

Committee:

____
Johannes J. Feddema, Chairperson

____
William C. Johnson

____
Stephen L. Egbert

Date approved: __July 27, 2007__________

Table of Contents

List of Figures

List of Tables

1. Abstract

Urbanization is a dramatic example of how people alter the surface of the Earth and have a significant impact on local climates. Understanding how urban characteristics interact with the environment on varying scales will help mitigate harmful changes to local and global climates. Localized urban influences on climate are well-documented, and logically it can be asked whether expanding urban areas influence global climate. In order to understand the potential effects of urbanization on global climates, urbanization must be included in global climate models. Furthermore, such a model will need global databases of urban extent and urban characteristics. This thesis describes the methods and characteristics of a dataset that can be used to simulate urban systems within global climate models. Specifically, the dataset represents three main categories of urban properties: spatial extent, urban morphology, and thermal and radiative properties of building materials.

2. Introduction

As people transitioned from hunting and gathering to agricultural societies, we began to significantly alter the surface of the Earth (Thomas 1956). Agriculture in turn allowed human settlements to become more permanent and eventually evolve into the urban centers of today. With industrialization and expansion of the use of impervious surfaces and materials that have significantly different thermal and radiative properties, cities began to modify their local climate resulting in urban heat islands (Oke 1987). The urban heat island effect is characterized by warmer urban areas compared to surrounding rural areas (Landsberg 1981, Oke 1987).

With the rapid growth of urban areas in modern society, it is likely that heat island effects are increasing locally and consequently globally. Presently, over half of the world's population lives in urban areas, and in Japan, Europe, and the U.S. at least 80% of the population inhabits urban areas (Elvidge *et al*. 2004). With more people migrating to urban areas, metropolitan areas are expanding world wide. Urban areas cover from 1-3% of the Earth's land surface, and their extent and intensity are expected to increase dramatically (CIESIN *et al.* 2004, Shepherd 2005). Accompanying the spatial growth of urban areas, there is an escalation in the use of heat-holding materials and human energy consumption, both potentially intensifying the urban heat island effect.

The rapid global urbanization rate necessitates the need for climate modelers to represent urban areas in global climate models (GCMs). Modeling how urban areas influence global climate will help scientists understand how to alter urban characteristics to lessen their impact on climate. In addition, as governments work to address global warming, policymakers will first look at areas where most people reside, our cities. If urban responses to climate change differ compared to the response in natural environments it is important that this differential response be included in climate impact assessment studies. In other words, the purpose of including urban systems in GCMs has two aspects. It is important to know how urban areas will be affected by climate change, but it is equally important to understand how urban areas might be contributing to climate change.

Previous research demonstrates that urban areas influence climate on a local scale via several mechanisms. These mechanisms lead to a greater capacity for heat absorption because of urban canyon geometry, heat storage in building materials, less evapotranspiration because of the increase in impervious cover and subsequent decrease in vegetation and latent heat fluxes, and the trapping of atmosphere-warming pollutants via temperature inversion (Oke 1982, Oke 1987, Oke *et al.* 1991).

Realizing a need for global urban modeling is a first step. However, any global scale modeling effort requires that the model be able to work for all places and in all seasons. Recent improvements in urban models allow them to capture these complexities, but they require an extensive global dataset of urban characteristics. Spatial characteristics and physical properties of urban systems vary widely due to cultural factors and the source of materials used to build the structures (Grimmond and Souch 1994, Grimmond and Oke 1999, Grimmond 2007). Therefore, there is a need for a global urban dataset that provides this information on urban spatial and physical properties that fit in with the required GCM parameters on a global scale. This thesis strives to answer the question: *What is the best methodology to represent urban characteristics on a global scale from a climate modeling perspective?* As part of this goal, a dataset was created that delineates urban areas and their properties across the globe.

This thesis describes the creation of a global database of urban characteristics evolved from the need to improve landcover data used in the Community Climate System Model (CCSM), a climate model currently used by the National Center for Atmospheric Research (NCAR). The Community Land Model (CLM) is the landcover component of the CCSM., requiring certain input parameters to effectively simulate urban influences on climate. Input parameters include three main categories: 1) spatial extent of urban areas, 2) urban morphology characteristics, and 3) thermal and radiative properties of building materials. These categories encompass the extent of the databases constructed for this thesis.

3. Background

Influences of landcover change on climate

With his book *Man and Nature* first published in 1864, George Perkins Marsh began the discourse on man's influence on nature, with special emphasis on land cover change. His work focused on human impact on the surface of the Earth, particularly relating to deforestation. Thomas (1956) presented a collection of works on the ecological consequences of human activities, including human use of fire to control the environment, the clearing of Europe's woodlands, the natural history of urbanization, and the limits of Earth's resources. Thomas (1956) also pointed out how wide-spread agriculture was a major factor in Earth's changing land surface. Wolman and Fournier (1987) studied the impacts of agricultural systems on atmospheric chemistry and air quality, soils, hydrology, and water quality in the mid 20th century. They concluded that human-induced "land transformation" has a far-reaching impact on these systems and that the effects are likely irreversible, at least for now. This work has since evolved into measuring agriculture's influence on the atmosphere, and on studies designed to mitigate the effects of carbon emissions from agricultural activities (Houghton *et al*. 1983, 1999, 2002, Turner 1990, Houghton and Hackler 1995, 2001).

In a related vein, the Intergovernmental Panel on Climate Change (IPCC) was established in 1988 to pursue research and provide information to the public and policymakers about how human activities influence climate (IPCC 2007). The IPCC has produced four Assessment Reports on the state of the global climate and likely causes of change. Initially, claims by the IPCC that climate change was to a degree human-induced were hotly debated, but in recent years the claims have been generally accepted. IPCC's most recent Assessment Report (AR4) acknowledges the influence of land cover change on global climate, but goes no further in studying land cover change in this context (IPCC 2007).

Land use and land cover change are intrinsically linked to weather and climate through many mechanisms. Links between the two include exchange of greenhouse gases, energy exchanges through the radiation balance (solar and long-wave) and aerodynamic energy exchanges in the form of sensible and latent heat fluxes, and through alteration of topography and roughness of surface features. As humans continue to alter the surface of Earth, we continue to alter the dynamics between land and atmosphere. While surface characteristics affect local climate, a changing climate also affects the land surface. Because of this duality, the study of land cover change and its related feedbacks with the atmosphere is an important component of understanding global climate dynamics.

Influences of urbanization on climate

Urbanization is one of the most dramatic types of land cover change. Not only does it influence climate directly through temperature changes (*i.e.* urban heat island), but it also modifies the hydrology, vegetation, wildlife habitat, and biogeochemical exchanges of a location. NASA scientists estimated that one-third to one-half of Earth's land surface has been altered by human development (2005).

On a city scale, scientists first acknowledged how changing from rural to urban land cover influenced climate in 1820 London. Luke Howard observed that the city was 2.1°C warmer in the daytime than the adjacent rural areas, a phenomenon later described as the urban heat island. Howard also noted that the effect is more dramatic at night, as buildings and pavement release stored heat (Landsberg 1981).

The extent of an urban heat island is related to population (Oke 1982, Viterito 1989). Specifically, the difference in temperatures of urban and adjoining rural areas increases as a logarithmic function of population (Bonan 2002). City size and population largely dictate heat island extent as people tend to create environments that store and release heat. For instance, since impervious surfaces such as roads, buildings, and sidewalks cover soil, a source of water vapor, there is a reduced latent heat flux. Additionally, the materials that make up the impervious surfaces (*e.g.* asphalt) store heat, thereby storing, redistributing and typically increasing sensible heat flux to the atmosphere (Grimmond and Oke 1995).

Impervious surfaces are a main driver of heat islands, but heat island development and intensity are subject to weather conditions. The greatest temperature differences between urban and nearby rural areas generally occur on clear, calm evenings while minimum heat islands occur under cloudy and windy conditions (Kidder and Essenwanger 1995). Wind helps mix adjoining air masses and reduces the thickness of the urban boundary layer, thereby reducing the urban heat island effect.

Within-city temperature variations can be attributed to topography, proximity to bodies of water, type of building materials, and differences in land use including density of development and the amount and types of vegetation present. One study found that land use accounted for 17-25% of air temperature variations within Lawrence, KS (Henry *et al.* 1985, Henry and Dicks 1987). Similar studies using high-resolution satellites confirm these findings by determining that commercial-industrial areas are warmer while parks have cooler temperatures (Carlson *et al.* 1981, Vukovich 1983, Roth *et al*. 1989, Nichol 1996).

Theoretical studies and satellite studies highlight the urban characteristics that lead to heat islands. First, the morphology of urban areas, or the size, shape, and orientation of the physical components explain in part the temperature contrast with adjoining rural areas. Additional alteration of the surface response depends on the physical properties of these factors, subdivided into thermal properties (*i.e.* heat capacity, thermal conductivity) and radiative properties (*i.e.* emissivity, albedo), which merge to account for temperature differences. The combined morphology and physical properties of urban areas account for the differential radiation balance at the surface compared to surrounding rural neighborhoods. These factors also account for storage of heat in urban materials as well as the division of energy into latent and sensible heat (Landsberg 1981, Oke 1982, 1987, 1988a, 1995). Because of the complexity of these interactions, modeling urban climatology faces many challenges, particularly when working at the global scale.

Previous efforts to model urban climatology

Modeling theory in urban-climate interactions has undergone several advances since Oke published an initial review of urban climatology (1974). Prior to this time, studies were focused primarily on measuring and describing heat island properties fueled by increasing concern over how the urban environment influenced humans (Oke 1974, Landsberg 1981). Since Oke's (1974) review, modelers began to consider urban systems in terms of individual buildings, horizontal surfaces between the buildings, and their interactions (Arnfield 2003). Individual buildings, with their wall and roof facets, each experience varying time exposures of solar radiation, net longwave radiation exchange, and ventilation (Arnfield 1984, 2000, Paterson and Apelt, 1989, Verseghy and Munro, 1989a, 1989b). Impervious surfaces (*e.g.* sidewalks and roadways) and pervious surfaces (*e.g.* lawns and gardens) comprise horizontal surfaces, which have distinct properties including radiative, thermal, aerodynamic, and hydrological elements (Oke 1979, Suckling 1980, Doll *et al.* 1985, Asaeda *et al.* 1996, Anandakumar 1999, Oke 1989, Grimmond *et al.* 1996, Kjelgren and Montague 1998).

Fundamental units of urban systems can be aggregated hierarchically (Arnfield 2003). Walls of buildings and the surrounding horizontal surfaces define the urban canyon (Figure 1). This fundamental morphological urban unit can be scaled up to include urban canyons and roofs of adjacent buildings (city blocks). City blocks make up neighborhoods, etc until reaching the scale of the entire city.

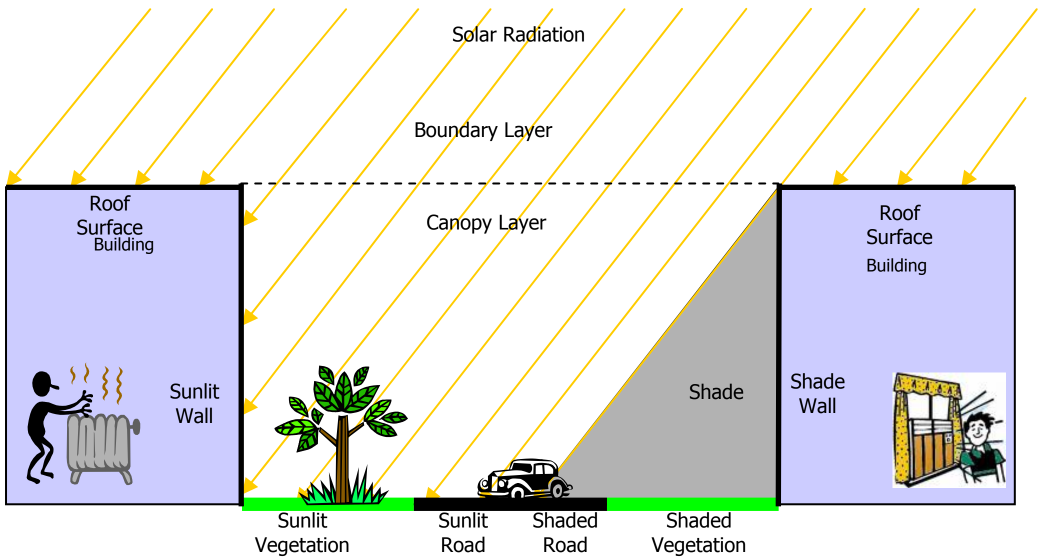

Figure 1. Urban canyon concept. Note that the urban canopy layer is defined by the height of the buildings.

Matters of scale and related complexity of urban systems has been a challenge to modelers. Model developers have created detailed maps of urban morphology (Ellefsen 1990-91, Grimmond and Souch 1994, Cionco and Ellefsen 1998) or have taken the approach of observing urban systems at aggregate scales, such as the objective hysteresis model by Grimmond *et* *al*. (1991). This model focuses on aggregate heat storage responses to net radiation forcing of several surface types depending on the spatial extent of each surface. Other models use the urban canyon concept (Figure 1) to incorporate mutual interactions of the combined budgets of constituent facets (Terjung and O'Rourke 1980a, 1980b, Mills 1993, Arnfield 2000).

The urban canyon's varied surfaces each possess a unique energy balance that influence neighboring surfaces as they interact (Arnfield 2003). Individual energy budgets interact with those of same-scale adjacent units by reflection of shortwave radiation, exchanges of longwave radiation and by exchange of convective energy balance terms through advection (Arnfield 2003).

Energy input into the urban system is based on the amount of net radiation (Q^*), which is a result of the all sources and losses of solar and terrestrial radiation to and from a surface. It is represented by

$$Q^* = S\downarrow(1-r) + L\downarrow + L\uparrow$$

where $S\downarrow$ represents incoming solar (shortwave) radiation, and r represents the average surface albedo or reflectivity, thus $S\downarrow(1-r)$ represents absorbed radiation. $L\downarrow$ equals incoming longwave radiation from the atmosphere, and $L\uparrow$ represents outgoing longwave radiation from the surface. Radiative interactions in the urban canyon are intrinsically linked to reflections caused by the geometry of the canyon and external radiative sources. Based on energy input to the system the basic surface energy balance is characterized by

$$Q^* = Q_H + Q_E + Q_G$$

where Q^* equals net radiation, Q_H equals turbulent flux of sensible heat, Q_E equals turbulent flux of latent heat, and Q_G is conductive heat flux into or out of a surface (Arnfield 2003).

To consider energy fluxes at a larger scale, or for total urban landscapes, it is useful to consider a different concept for the energy budget for an imaginary volume of the urban canyon, which extends from below the ground level surface up to roof level, at the upper margin of the urban canopy layer (Oke 1988). This energy budget (Figure 2) is represented by

$$Q^* + Q_F = Q_H + Q_E + \Delta Q_s + \Delta Q_A$$

where Q_F represents anthropogenic sources of energy (*e.g.* motor vehicles, house furnaces, power plants, human metabolism), ΔQ_s is the storage heat flux (*e.g.* within air, trees, building materials, soil, etc.), and ΔQ_A is the net advection through the sides of the imaginary volume (Arnfield 2003). Anthropogenic sources of energy (Q_F) such as can be quite large, and in extreme cases may be of similar magnitude as net radiation (Grimmond and Oke 1991, Schmid *et al.* 1991, Ichinose *et al.* 1999).

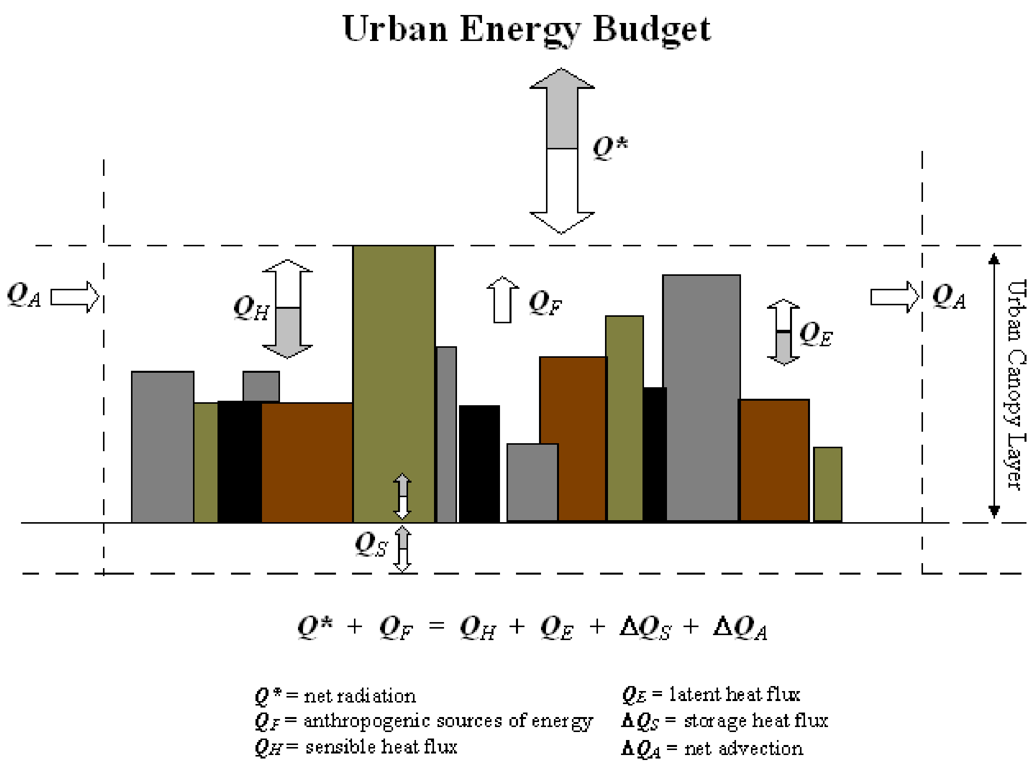

Figure 2. Urban energy budget. Urban areas are warmer due in part to anthropogenic energy sources.

Because ΔQ_s is generally believed to be a large part of net radiation, ways to parameterize ΔQ_s have been sought for use in energy balance studies of urban systems (Arnfield 2003). One study concludes that thermal factors and canyon geometry are the most important parameters (Arnfield and Grimmond 1998), which agrees with other findings (Oke 1995, Sailor and Lu 2004, Oleson *et al.* 2007b).

In computing these radiation exchanges, one must look at skyline obstructions to assess shading impacts (*e.g.* sun-lit versus shaded wall) (Frank *et al.* 1981a, b, Arnfield 1982a, 1984) and view factor relationships

(Figure 3) within the canyon that control the relative exposure of one surface to another (Steyn 1980, Johnson and Watson 1984,1985, Steyn and Lyons 1985, Steyn *et al.* 1986, Watson and Johnson 1987, Chapman *et al.* 2001, Grimmond *et al.* 2001).

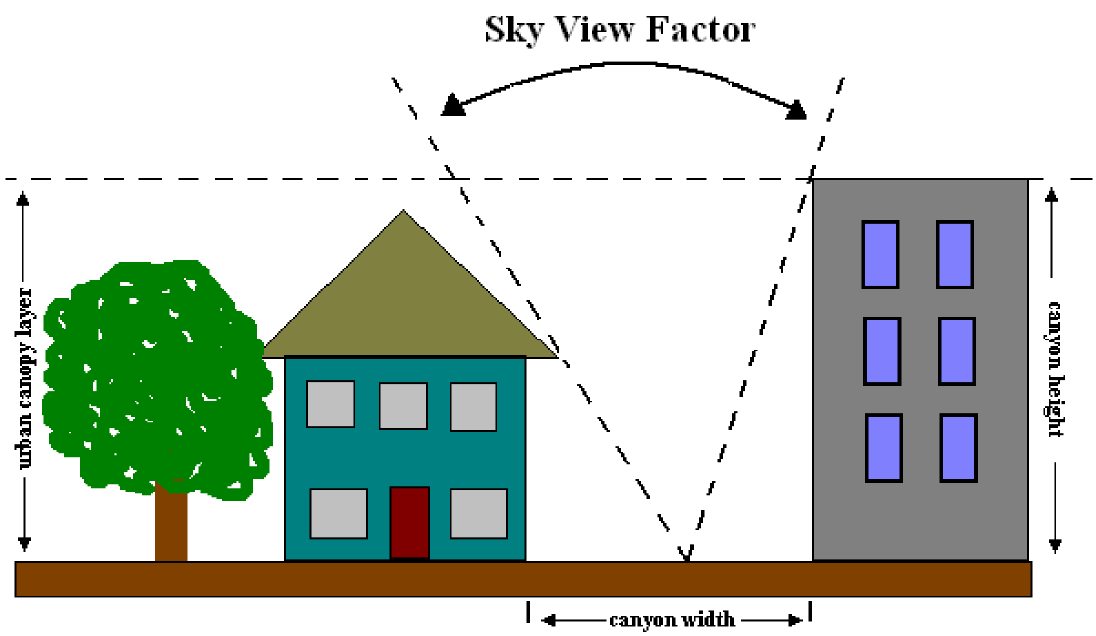

Figure 3. Illustration of sky view factor, defined by Oke (1997) to be the fraction of overlying hemisphere occupied by sky. Figure adapted from Oke (1997).

Another important consideration in urban models is the water balance. Water availability is a major controlling factor in the disposition of energy from a surface. The lack of water at the surface reduces latent heat fluxes and thereby forces increases in other energy balance disposition terms. In addition it affects atmospheric conditions because of decreased latent heat and increased sensible heat causing urban systems to have a larger Bowen ratio (i.e., the ratio of sensible to latent heat) than adjoining rural areas. (Yap and Oke 1974, Oke 1979, Kalanda *et al*. 1980, Oke and McCaughey 1983, Cleugh and Oke 1986, Oke and Cleugh 1987, Grimmond 1992, Roth and Oke 1995). Sensible and latent heat fluxes due to water depend largely on the amount and type of surface, whether it is an irrigated lawn or wet road, for instance. Because of reductions in available water supply on most urban surfaces, latent heat flux is typically reduced, resulting in higher surface temperatures to drive other energy disposition processes.

To summarize the state of knowledge for modeling urban systems, modelers have found that the urban canyon concept captures the morphological parameters of the system, and that information about the facets, surfaces, materials, anthropologic influences, and hydrology are all important aspects needed to replicate the observed energy balance relationships in an urban system. The relative importance of any factor depends largely on the scale of the model, but studies have found the most important factors to be thermal and morphological parameters. These urban characteristics must effectively be represented in order to measure an urban system's influence on climate.

When considering the development of a model that operates on a global scale, a number of factors must be considered, including computational efficiency of the model and its ability to simulate urban systems in a wide variety of climates. Early attempts to consider urban factors in land surface models had several limitations. There have been three major types of urban parameterizations: 1) empirical models, 2) vegetation models adapted to represent the urban canopy, and 3) single-layer and multi-layer models that represent the urban canopy in three dimensions (*e.g.* urban canyon type models; Masson 2006).

Empirical models (*e.g.* Grimmond *et al.* 1991) look at observed data for a short duration to derive a statistical relationship representing urban responses to climate input variables. By relying on statistical relations during the observed period, the models are limited to the specific range of conditions present at that time. Vegetation models were not developed to capture urban characteristics (*e.g.* energy storage in the urban fabric), so they must be adapted to represent urban areas effectively (Taha 1999, Atkinson 2003, Liu *et al.* 2004, Best 2005). Finally, single-layer and multi-layer models best represent urban systems in three dimensions, but are the most complex and require greater computing resources (Masson 2006).

Some argue that the simpler approaches of the empirical and adapted vegetation models are all that is needed to represent urban areas on a global scale arguing that the global model scales up the data to a coarse grid, so fine details may be lost (Taha 1999). However, another limitation of the simpler approaches is that they do not consider significant physical parameters such as heat storage. For instance, building materials store heat, and densely placed building structures also trap heat, so construction materials and geometric form of urban areas play a large role in the magnitude and temporal characteristics of urban heat islands (Oke 1995, Sailor and Lu 2004). These factors are included in the three-dimensional, single and multi-layered models. Furthermore, the more complex models offer more options to test hypotheses that include morphologic and building properties as part of testing mitigation proposals, etc.

The second reason for implementing a three-dimensional urban canyon model is that this model can better simulate the effects of climate change in urban areas. Including specific urban climate simulations within a GCM (*i.e.* simulations within urban areas) allows us to better assess the impact of climate change on urban populations, which encompass over half the world population today and are projected to include about 65-70% of all people by 2050 (CIESIN *et al.* 2004, Shepherd 2005). Distinguishing urban and non-urban areas allows scientists to overcome differing sensitivities to climate change of these areas and to determine how urban areas will be influenced by changing climate (Best 2006). For these reasons NCAR developed a single-layer, three-dimensional urban model to answer questions about urban-climate interactions.

4. Model description

The National Center for Atmospheric Research (NCAR) Community Climate System Model (CCSM) is a state-of-the-art computer model that simulates Earth's past, present, and future climates. CCSM is made up of four major components which include models of energy and water transport and exchange in the atmosphere (CAM), oceans (POP), land (CLM) and sea ice (CSIM). Urbanization represents one potential human impact on land cover change, a process represented in the CLM. (Figure 4).

The CLM considers interactions between the atmosphere and different ground cover, including glaciers, lakes, soils, vegetation, and urban areas. The model takes into account land surface and atmospheric inputs, then calculates heat and radiation fluxes, temperature, humidity, and moisture values, river flow, volatile organic compound emissions, and CO_2 fluxes. Included in the CLM are two sub-models. A global vegetation model simulates what types of plants are present and where these plants grow as a function of climate (Sitch *et al.* 2003). Also, a sub-model simulates interactions between the atmosphere and urban areas (Oleson *et al.* 2007).

In the CCSM, Earth's surface is divided into grid cells approximately at a resolution of 1.4° (and will potentially be improved to 0.5° or smaller in the near future). Each grid cell has the capacity to be unique. For instance, within the CLM, each grid cell is represented by a nested sub-grid hierarchy including land units, plant functional types (PFTs), and snow/soil columns (Oleson *et al.* 2004). Within these limits, a CLM grid cell may contain any number of land units, PFTs, or snow/soil columns.

The five land unit types are glacier, wetland, lake, vegetation, and the newest addition, urban. Urban is now included to account for increasing extent of urban landcover, which occupies a significant fraction of some grid cells (Oleson *et al.* 2006). Only vegetation and urban classes can be further subdivided. Vegetation is divided into PFTs while urban is subdivided into three levels of urban: tall building district, high density commercial/residential and low density residential.

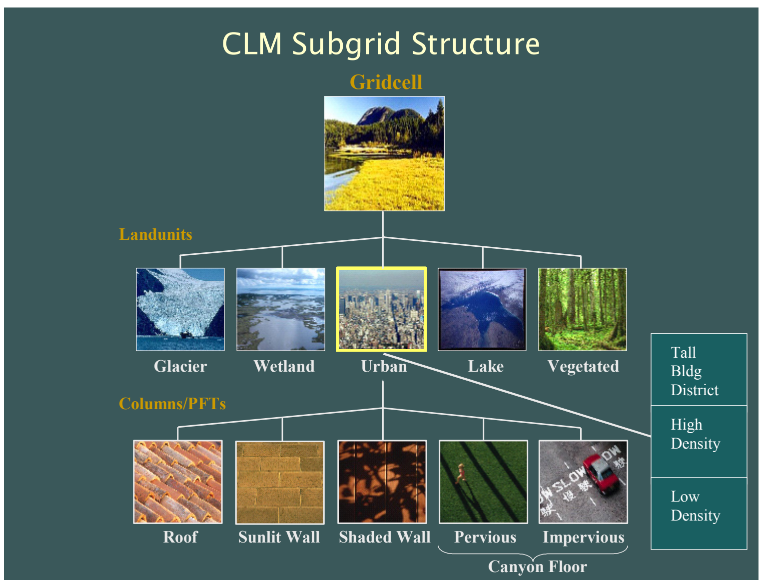

Figure 4. The urban landcover is a new subgroup of the landcover grid cell Adapted from Oleson *et al.* 2006.

The urban sub-model, herein referred to as CLM-Urban, uses the urban canyon concept to calculate interactions between urban areas and the atmosphere (Figure 5). Therefore, as shown in Figure 4, the sub-model requires information on roofs, walls, and the canyon floor including impervious and pervious surfaces. In contrast to the accepted definition of an urban canyon, the urban canopy layer of the model extends just above the height of the buildings to account for air mixing above the buildings (Oleson *et al.* 2007a). Processes may occur here such as latent and specific heat fluxes due to ponded water or snow. The model's lower boundary follows the traditional definition of an urban canyon, as it extends down to the depth of zero vertical heat flux in the ground (Oke 1987).

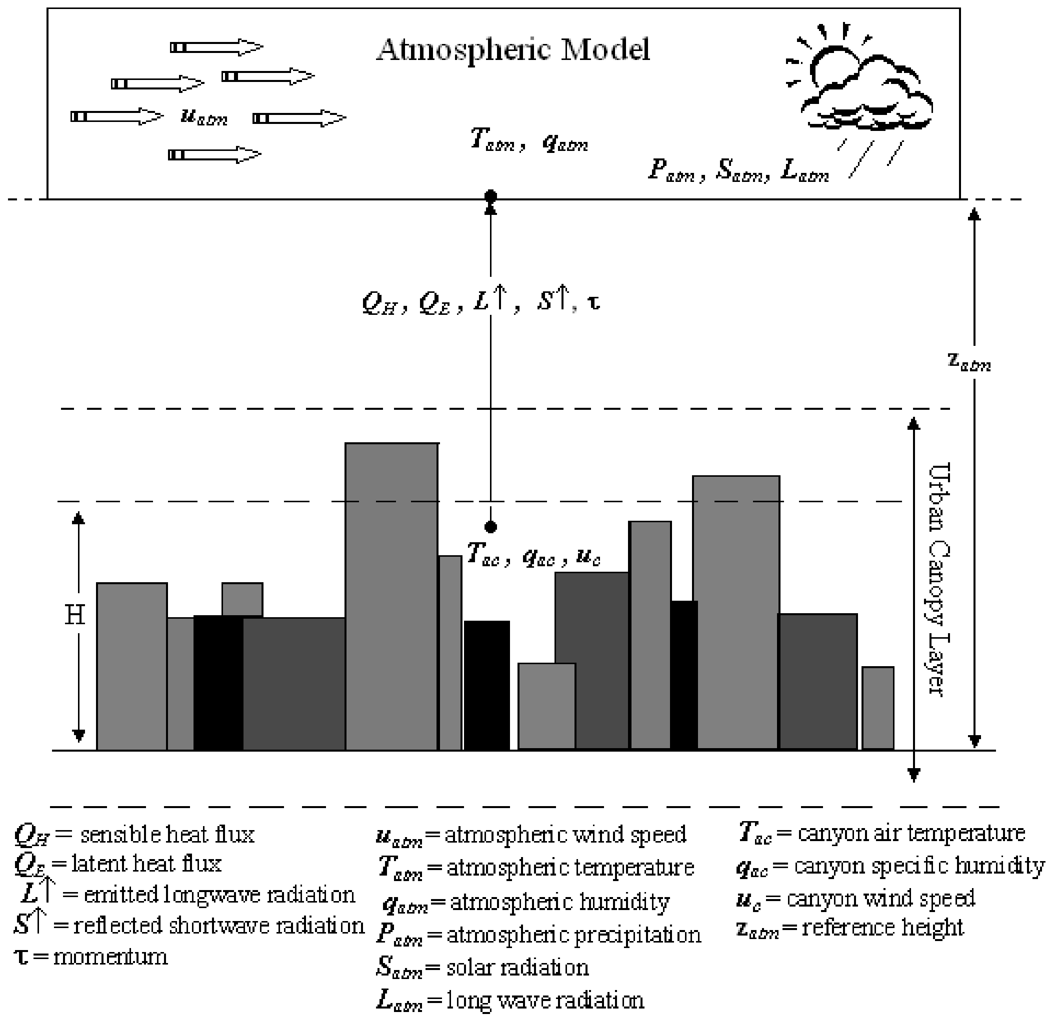

Figure 5. Interactions between the atmospheric model and the urban canopy model. The urban model is forced by the atmospheric model by wind speed, temperature, and specific humidity. The urban model returns information to the atmospheric model as sensible and latent heat flux, emitted longwave radiation, reflected shortwave radiation, and momentum (Oleson *et al.* 2007a).

The model also accounts for orientation of the canyon to consider changes in incoming solar radiation as the sun moves across the sky. In other words, the model integrates incident radiation for all sun angles for all the walls (*i.e.* walls are rotated through time to take into account the total radiation for all aspects at each time step). This is to simulate the idea that streets can have any orientation.

CLM-Urban (Figure 6) simulates 1) absorption and reflection of solar radiation, 2) absorption, reflection, and emission of longwave radiation, 3) momentum, storage, sensible, and latent heat fluxes, 4) anthropogenic heat fluxes due to traffic and waste heat from building heating/air conditioning, 5) heat transfer in roofs, building walls, and the road, and 6) hydrology (Oleson *et al.* 2007a).

The urban sub-model is forced by the atmospheric model by atmospheric wind, temperature, specific humidity, precipitation, solar radiation, and long wave radiation. These conditions influence the outcome of CLM-Urban simulations. CLM-Urban models the aforementioned processes, and returns information to the atmospheric model including sensible and latent heat fluxes, emitted longwave radiation, reflected shortwave radiation, and momentum. CLM-Urban calculates air temperature, specific humidity, and wind speed within the urban canyon. These interactions are illustrated in Figure 5. Fluxes from each canyon surface interact via a common air mass that represents urban canopy layer air (Oleson *et al.* 2007a). The flux information provided to the atmospheric model by CLM-Urban is averaged with whatever other landcover is present in the same grid cell. Then the area-averaged fluxes are used by the atmospheric model in the next time step (Oleson *et al.* 2007a).

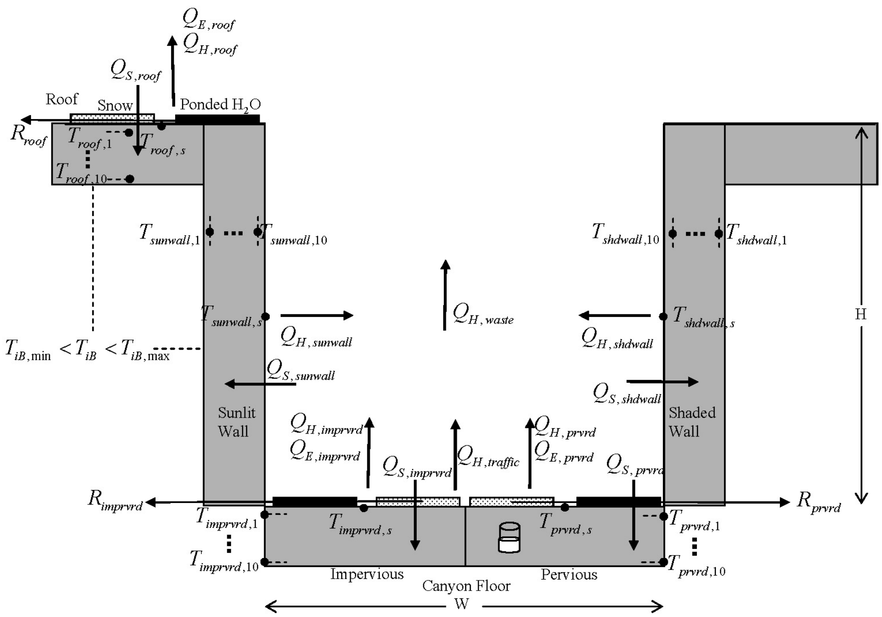

Figure 6. NCAR urban model (CLM-Urban) with specific components illustrated. Symbols follow those described in Figure 5 (Oleson *et al.* 2007a). Used with permission from the author.

CLM-Urban calls for morphologic, thermal, and radiative input parameters to efficiently simulate these processes. Morphologic parameters include height-to-width ratio of the canyon, building height, roof fraction (as a percent of total area), pervious canyon floor fraction, roof and wall thicknesses, and impervious canyon floor thickness. Thermal properties include thermal conductivity and volumetric heat capacity for roofs, walls, impervious and pervious canyon floor materials, minimum and maximum interior building temperatures, and soil texture. Radiative properties are emissivity and albedo of roofs, walls, and impervious and pervious canyon floor materials.

This information allows the model to effectively capture the character of an urban area. Considering how cities across the globe vary widely in terms of building materials and structure of cities (*i.e.* different canyon widths, different building heights), these parameters successfully portray the variances in these factors from region to region and even between urban categories (*e.g.* tall building district versus low density residential).

CLM-urban has undergone a number of sensitivity tests to determine which parameters have the greatest influence on results. Model developers used existing data from Vancouver, Canada (Oke *et al.* 1999) and Mexico City (Voogt and Grimmond 2000) to determine how well the model performed in simulating urban heat islands in these dissimilar environments (Oleson *et al.* 2007b). By adjusting the data values up or down from the actual numbers, the study also determined which model parameters were most sensitive to perturbations. Results determined that the model is most sensitive to heat storage and sensible heat flux. For this reason it is important to accurately record the morphology and thermal properties for inputs into the model.

In addition, the model effectively simulated temperature changes associated with urban heat islands, such as the decreased range in diurnal urban temperatures compared to surrounding rural areas and an increase in intensity of heating with increased height-to-width ratios. The success of the sensitivity tests show that CLM-Urban will be effective in studying urban climate processes within GCMs (Oleson *et al.* 2007b).

5. Methods

The initial idea for this project was generated by Johan Feddema, of the University of Kansas who was developing methods for introducing human impacts in the CCSM. To introduce urban areas into the CCSM a global dataset characterizing the extent of urban areas and urban properties was needed. He developed the three-step process of 1) diving the world into manageable pieces with similar urban characteristics, 2) determining the spatial extent of urban areas (along with the three levels of urban density), and 3) compiling a database of building properties for each of these categories within each region. When we began, no one to our knowledge had taken on a project such as this before. Therefore, developing the details of the methodology proved to be a continuous creative process.

CLM-Urban requires certain input parameters to efficiently simulate urban interactions with the atmosphere. A model validation study showed that heat storage and sensible heat flux were quite sensitive to morphological and thermal parameters (Oleson *et al.* 2007b). These parameters comprise the dataset to be created for this project, including spatial extent of urban areas, canyon height-to-width ratios, building height, thermal properties for roofs and walls (specific heat and thermal conductivity), and radiative properties (emissivity and albedo) for roofs and walls.

Defining urban extent

When considering urban areas on a global scale, it is apparent that regional cultural and physical characteristics control the nature of urban fabrics and the design of cities (Givoni 1976). Therefore, the first step involved dividing the world into regions with similar urban characteristics (Fig. 5). Similar urban characteristics can be determined by physical geography (including climate and available building materials (Givoni 1976, Olgyay 1992)) and culture (Clarke *et al.* 1989). South America is divided into three regions: tropical, temperate, and Brazil. Although Brazil shares similar cultural attributes and building materials with neighboring states, the country's urban areas are concentrated on the eastern coastal area of the continent. Because coastal cities attract tourism and have different structural requirements (*e.g.* to withstand high winds), coastal cities in Brazil differ significantly from their inland neighbors. Furthermore, the economy is more robust (Becker and Egler 1992), allowing for greater potential use of advanced building techniques and materials. Tropical and temperate South America regions differ mostly in climate, and urban buildings are built to accommodate the associated climate extremes. After conducting a similar evaluation of each continent for these factors, thirty three regions emerged with similar urban traits.

In the case of the United States cities often have a similar spatial pattern, likely due to the newness of urban centers compared to other regions such as Europe (Attoe 1988). They typically have a relatively small tall building district surrounded by commercial areas and dense residential buildings. This dense urban area is usually surrounded by extensive suburban areas. Because of varying geography, assorted building materials are available in different regions and diverse climates call for distinct structure types (Attoe 1988). Therefore, the contiguous U.S. was broken down into six regions to account for these variations. This process was repeated for the remainder of the globe, with the exception of Antarctica, which is not considered.

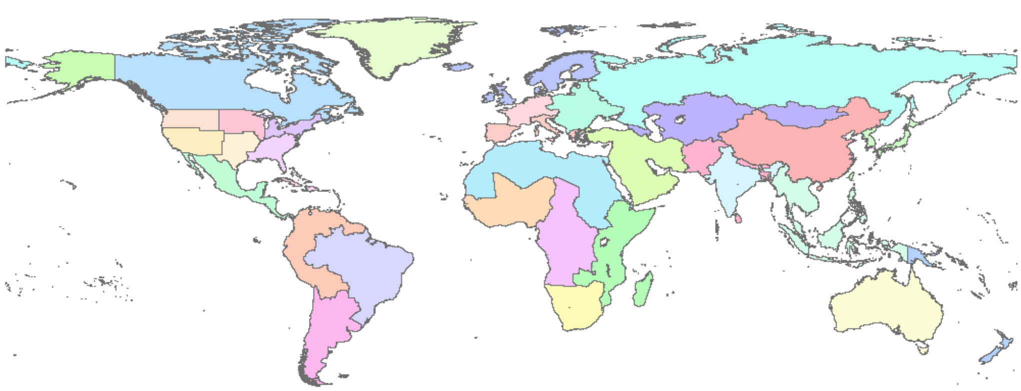

Figure 7. Thirty-three regions with similar urban character. Delineating factors include climate and housing characteristics.

Once the globe was divided into manageable portions, each region was examined individually to determine urban extent. Several satellite-derived landcover products are available and were evaluated for possible use to represent urban extent for this project (*e.g.* MODIS, GLC2000, and DISCover). However, these products show significant disagreement on the location and size of urban areas around the world. Moreover, CLM-Urban calls for three levels of urban intensity, which none of the satellite products provide. Because of these shortcomings in the satellite products, the LandScan (Dobson *et al.* 2000) population dataset was used as a proxy to define urban boundaries. Population density is not a perfect determinant of urban areas, but because of the ease of transition to temporal usage, it can answer more questions than a snap-shot of urban areas. As new population datasets emerge, they will lengthen the time series of population densities, and therefore can illustrate how urban areas evolve over time.

LandScan 2004 (Figure 8) shows where people most likely reside based on slope, landcover, nighttime lights, proximity to roadways, and census data (Dobson *et al.* 2000). Therefore, population densities calculated from LandScan values were used to define the boundary between urban and non-urban areas, and degrees of urban intensity. This was accomplished by setting a lower limit of population densities. For example, in the U.S. many suburban areas take on more rural characteristics where the density falls to less than 75 people per square kilometer. Thus, the urban boundary for many U.S. regions is near this value.

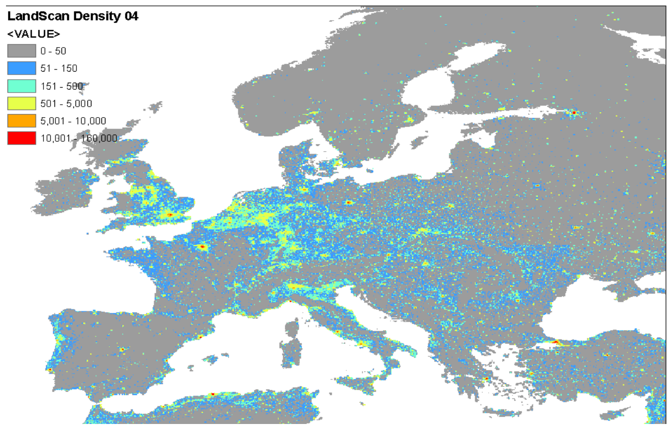

Figure 8. Population density of Europe based on LandScan 2004 (Oak Ridge National Laboratories 2005). Values are in people/km^2.

Once urban areas were defined, the areas were further delineated into three categories, including tall building district (TBD), high density commercial or residential (HD), and low density residential (LD). These categories best capture the structure of most cities in the world by taking into account different types of urban areas, while still maintaining a manageable level of complexity. Each region contains urban areas that can be represented by these categories, although specific thermal and radiative properties may differ between regions within a category. Therefore, individual regions were considered independently to determine boundaries of the three urban categories within the region.

Just as the lower limit of population density to define urban areas varies from region to region, the boundaries between urban categories differ also. Boundary assignments were made based on population density and observations of satellite imagery in at least ten cities for a given region (Appendix A). By studying images of populous areas from Google Earth and comparing them to the LandScan population density (Dobsen *et al.* 2000), natural boundaries typically presented themselves. In many cases, density values between neighboring pixels would present a large disparity corresponding to a change in urban density as seen in satellite imagery.

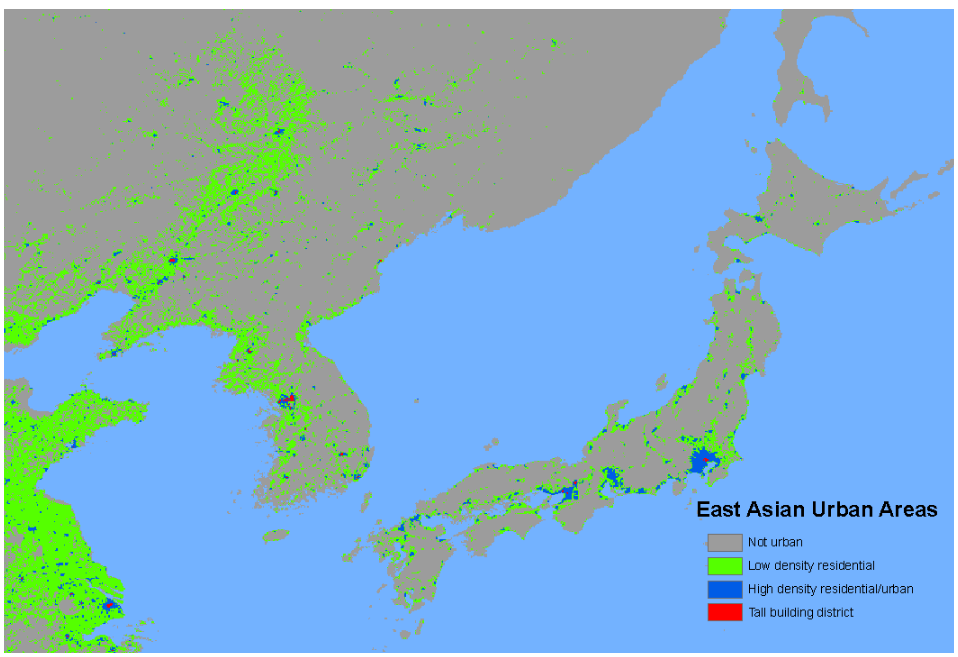

Figure 9. Urban areas of East Asia. Japanese cities are very densely built, with a much larger high density area than is typically found in the U.S.

Google Earth satellite imagery comes from a variety of sources (*e.g.* TerraMetrics, NASA, DigitalGlobe), and the available resolutions vary as well, from less than one meter (DigitalGlobe 2007) to 15m in most cases (EarthSat 2007). For a given region, cities with higher resolution imagery were sought out to get the best representation of urban areas for that region.

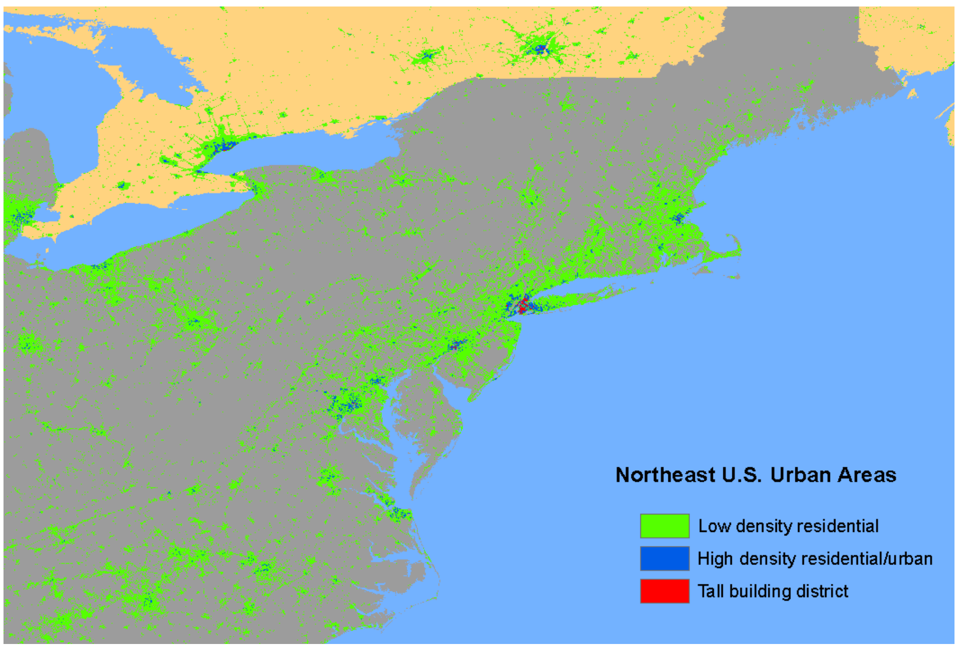

Figure 10. Viewing urban areas of the Northeast U.S. shows that New York City is easily discernible as the largest metropolitan area due to its large TBD.

Although it is recognized that urban areas within regions vary widely, multiple cities ("validation cities") within a region were compared to find typical regional population threshold values. Boundaries were initially assigned based on one city, then adjusted to fit subsequent cities within a region. Finally, the initial city or cities studied were revisited to ensure any adjustments still effectively represented all or most cities within the region. The selection of cities used to define boundaries was based on three main factors: relatively dense population, location (cities were selected throughout region to be representative of entire region), and availability and resolution of imagery.

For consistency, definitions for each category are kept in mind during this process, especially when initially assigning boundaries. Tall building districts, commonly referred to as central business districts, are defined for the purpose of this study as groups of buildings at least one square kilometer in extent that are a minimum of ten stories tall. High density commercial or residential areas are defined as groups of buildings from three to ten stories tall, and with a high percentage of impervious cover. Low density residential areas contain buildings typically one to three stories tall, but they are more spread out and the area contains a relatively high percentage of vegetation or bare ground.

Once the urban boundaries were assigned for each region, an inter-region comparison looked at disparities on the global scale, and ensured that regions with similar qualities, such as the U.S. and Middle America were consistent in their definition of urban categories. Again, minor adjustments were made to dispense with outliers.

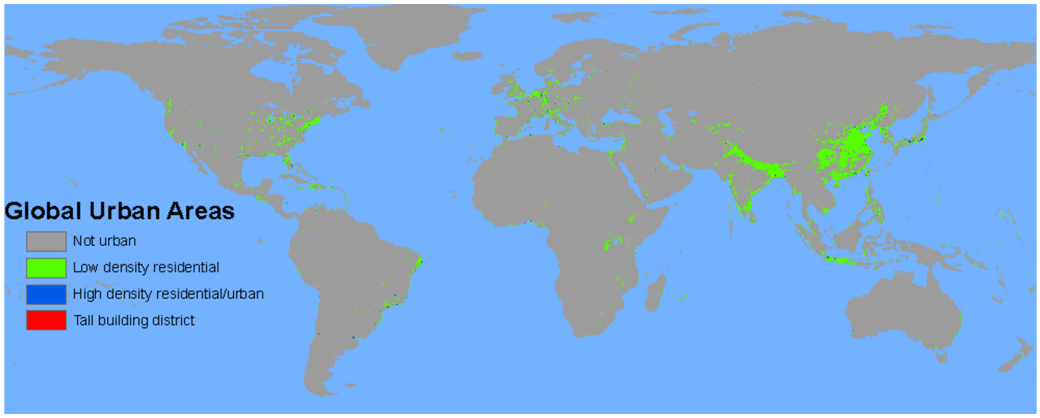

Figure 11. Global urban areas. Because of the scale, low density residential is the most visible category since it has the greatest spatial extent.

Determining urban morphology characteristics

a. Building heights

Urban category definitions (TBD, HD, and LD) must be adaptable to any given location. The least dense category in the U.S. generally identifies suburbs, but in places such as northern Europe, the category encompasses two-story, densely-packed homes. Because the categories vary widely by region, it is necessary to additionally describe the form of the buildings at each locale. For instance, a tall building district in the U.S. northeast is much taller than a tall building district in tropical South America. This justifies the next step, determining urban morphology characteristics for the 99 regional categories (33 regions x 3 categories).

A first step in determining urban morphology included estimating average building heights and height-to-width ratios of the urban canyon within each regional category. A global database of tallest buildings by city was used to estimate average heights for tall building districts within each region (Emporis 2007). Where available, 25 of the tallest building heights were averaged for five cities within a region, then the average building heights of these cities were calculated to determine an average regional tall building value. This average was then decreased appropriately to account for the remaining buildings in the TBD (Table 2). Some regions either have no TBD (*e.g.* Greenland), or have few cities with a TBD (*e.g.* West Africa). In these cases, the maximum number of buildings in the Emporis dataset was averaged.

City	**Average of 25 tallest buildings (meters)**
Houston	208
Dallas	184
St. Louis	112
Kansas City	112
Oklahoma City	83
Average	140
Value used for TBD	**120**

Table 1. Average tallest building heights for five south-central U.S. cities.

For the high density category, imagery of the verification cities along with Emporis (2007) data was used. By viewing imagery of city skylines, building heights were estimated by comparing HD heights to the TBD. To further support the assessment, stories in buildings were counted so that heights could be estimated. Where available, the Emporis (2007) dataset was used, but it includes far less information about non-high-rise buildings and coverage is limited.

Low density building heights were determined primarily based on housing types. For instance, in the U.S. a typical two-story frame home is approximately 8 m tall. Local building codes and estimations from imagery supplement this method. Thus, once information was gathered about the types of buildings common in LD areas, building heights were evident.

b. Height-to-width ratios

Local building codes and other municipal documentation also helped determine appropriate height-to-width ratios. From these documents, conventional residential and commercial road widths were located. After determining an average road width for a regional category, building heights were used to calculate height-to-width ratios for the urban canyon (Figure 1). For instance, in a suburban area with two-story homes (8 m) with a 24 m wide canyon bottom (including road and lawns), the height-to-width ratio equals 0.33 (8m / 24m = 0.33). Where official documentation was lacking, road widths for many verification cities were found on the internet, typically as part of information necessary for emergency planners and other government agencies. Once widths were estimated for the 99 categories, the ratios were calculated.

Determining urban thermal and radiative properties

Urban morphology only considers the three-dimensional form of the urban canyon. Additional information about thermal and radiative properties of buildings is required to effectively capture urban interaction with climate at many scales (Bonan 2002). Buildings are the main component of the urban canyon, especially in terms of how their structure and materials influence the canyon's thermal and radiative balance. Therefore, a database of typical building types and their properties was created to fulfill the NCAR urban model requirements.

For the 99 different urban classes, the three most common building types and roof types were determined and their relative abundance was reported in percentage terms (*e.g. Walls*: 50% wood frame home, 40% brick home, 10% stone home; *Roofs*: 70% asphalt shingle, 20% ceramic tile and 10% wood shingle). To make informed decisions regarding what constitutes common building and roof types, background research was required in the building trade literature as well as documentation describing the historical and cultural determinants of typical buildings in a region today (Givoni 1976, Olgyay 1992, Straube and Burnett 2005). However, in many cases imagery and geographical knowledge played a large role in approximating the most common building and roof types. Based on this knowledge, a table of three wall types and three roof types was constructed for each regional category (Appendix B).

To estimate thermal and radiative properties of walls and roofs, a look-up table of typical construction material properties was created, including density, specific heat capacity, and thermal conductivity (Appendix C). CLM-Urban calls for volumetric heat capacity (Oleson *et al.* 2007a), which was calculated using density and specific heat capacity.

Next, a table was created listing the specific building materials used in the construction of each wall and roof type. CLM-Urban calls for 10 layers for roofs and walls (Oleson *et al.* 2007a), so each respective wall and roof type was broken into 10 layers with information on each layer's thickness. For roofs and walls with fewer than 10 components in the roof or wall assembly, a primary material was repeated for more than one layer. For instance, for mud homes, mud is the only building material, so mud was stated as the material for every layer. The sum of individual layer thicknesses equals the standard thickness of a mud home. Appendix D includes a table of roof and wall types, broken down into 10 layers each. Once a material was assigned to each layer, its associated thermal properties (Appendix C) were added to the table. Finally, the total wall thickness was summed (Appendix D). Information on wall and roof assemblies came from research entities such as Canada's National Research Council Institute for Research in Construction (*i.e.* Mukhopadhyaya *et al.* 2004) and from building trade resources like *Flat Roofs: Non-Residential* from Knauf Insulation (2005a).

Another component of the wall and roof types involves the surface properties, which determine the radiative properties of the buildings. For each wall and roof the outside surface construction material was listed. Using the building materials look-up table the values for albedo and emissivity were then assigned for each location (Table 2).

Material Categories	**Thermal Conductivity W/m*K**	**Volumetric Heat Capacity MJ/m^3*K**	**Albedo**	**Emissivity**
concrete (cast, reinforced)	1.90	2.10E+06	0.88	0.23
concrete, blocks (hollow)	0.86	7.81E+05	0.94	0.23
concrete, precast panel	1.28	2.12E+06	0.90	0.23
brick (reinforced)	1.10	1.61E+06	0.91	0.3
limestone	2.90	2.31E+06	0.86	0.28
granite	3.49	2.42E+06	0.68	0.33
sandstone	1.30	1.81E+06	0.79	0.35
mud or adobe	0.60	1.41E+06	0.90	0.35
wood, unpainted	0.14	1.05E+06	0.86	0.40
wood, painted	0.14	1.05E+06	0.84	0.38
siding (aluminum or vinyl)	0.70	2.38E+06	0.91	0.54

Table 2. Lookup table of thermal and radiative properties of selected construction materials (Clarke 2001, Straube and Burnett 2005, Mukhopadhyaya et al. 2003, Oke 1987, Omega 2007, Weast 1981, Wechsler and Glaser 1966, and Reagan and Acklam 1979). For property-specific citations, see Appendix C.

The final product includes a GIS-based global dataset of urban extent divided into the three urban categories. The 1-km resolution dataset is in geographical grid format. Associated data tables can be linked to the urban extent grid via region names. Tables included are: wall types, roof types, material properties, and a master table that shows three common building and roof types per regional category and their frequency (Appendices B-D).

6. Evaluation of final product

A major concern in constructing a database of this scope is identifying methods that result in a meaningful outcome. Although some data exist on urban extent and building materials, none exist uniformly around the globe. The methods used here are, to an extent, arbitrary. But one must keep in mind that this is a first attempt at characterizing a complex system on a global scale.

Dataset validation techniques

Several schemes could be utilized to validate this dataset. First, consider how best to validate the spatial extent of urban areas. Remote sensing provides many valuable tools for defining urban areas, whether through aerial photography or satellite imagery.

Several data processing techniques exist to create useful datasets from satellite images. For example, supervised classification allows the person viewing the images to teach the computer how to delineate similar areas, such as urban landcover (Campbell 2002). One particular method has evolved recently particularly for the purpose of delineating urban areas. Called "boosting," this process improves supervised classification accuracy by providing a channel for integrating several datasets in the supervision and by using a base learning algorithm (*e.g.* a decision tree) (Schneider *et al.* 2003). The Moderate Resolution Imaging Spectroradiometer (MODIS) landcover team used boosting to delineate urban areas on the continental scale using LandSat images, Defense Meteorological Satellite Program's (DMSP) nighttime lights, and gridded population data (Schneider *et al.* 2003). Ongoing work to improve the MODIS urban classification involves further development of this strategy (Schneider 2007). The forthcoming dataset will include two levels of urban intensity. It will be important to measure the agreement between MODIS urban areas and the urban extent dataset as a validation technique.

Another classification scheme involves unsupervised classification using clustering algorithms. Clustering, which simply means the grouping of statistically similar features, can be used to discover rural-urban boundaries through edge-detection or other algorithms (Campbell 2002). Again, (*e.g.* hierarchical) clustering can be used to divide levels of urban intensity within the constrained "urban" area (Campbell 2002). Even though many clustering techniques have been successful at defining urban areas, it is an involved, time-consuming process, especially if applied at the global scale. For these reasons, it is appropriate to use this method as a validation technique, but perhaps not a dataset-building technique, due to the scope of this project.

Other remote sensing technology such as LIDAR (light detection and ranging) can also effectively identify urban boundaries. LIDAR works by bouncing a laser from an active sensor on an aircraft. The return signal precisely tells the sensor how far away the target object is (Campbell 2002).

Some urban areas have already been mapped with LIDAR, but due to time constraints and expense, this is not feasible at the global scale at this time. Nevertheless, cities with LIDAR coverage can be compared to the urban extent dataset to monitor how well it captures the three levels of urban in those cities.

Another remote sensing capability worth mentioning is radar. RADARSAT-1 and RADARSAT-2 are synthetic aperture radar (SAR) sensors that have the capability of providing high resolution coverage of urban morphology (NRC 2006). Like LIDAR, the technology involves the use of active sensors, which bounce signals off of the surface of interest, measure the time it takes for the return signal, and can then illuminate certain surface features, such as size, shape, and even texture (Campbell 2002). In this way it can effectively define urban areas including levels of urban intensity (Quattrochi and Weng 2006). In addition, because these satellites continue to collect data, there is an opportunity to monitor how urban areas change over time. Like existing LIDAR cites, cities that already have been mapped by these satellites can be compared to the urban extent dataset for another source of validation.

The urban landcover products available use a wide array of methods and remotely sensed imagery to define urban areas. However, there are major limitations of these datasets were discovered in evaluating data sources for this project. During this process, it was determined that the available satellite products should not be used in CLM-Urban because they do not effectively map urban areas throughout the world (*e.g.* GLC2000, MODIS, IGBP). Individual products showed inconsistent coverage of urban areas, and when product to product comparisons were performed, there was little agreement between the placement and extent of urban areas. These shortcomings prevent satellite products from being used as the global urban dataset for this project, but allow their limited use for validation purposes.

Validation of the building properties database presents its own set of challenges because it makes regional generalizations. Built into the methodology are ways to simplify building information, such as by incorporating consumer trends as reported by the National Association of Home Builders (2003). To continue to improve the database requires continued research of available building data, especially in less-studied areas such as Africa.

A final method for validating the morphological characteristics in the dataset is to compare it against site-specific studies. Site-specific information is available from individual works such as Grimmond and Oke's (1999) comparison of seven North American cities, and from more detailed studies for Vancouver (Oke *et al.* 1999) and Mexico City (Voogt and Grimmond 2000). These latter studies were completed with modeling urban climatology as a goal, so the data fit well into CLM-Urban. By completing test runs for these specific sites and for their respective regions, it is possible to determine how well the generalized data compares to the site-specific data.

Limitations of the data

Using population density to define urban boundaries presents a problem when attempting to include urban areas like industrial complexes and airports. With sparse population in these pixels, they are typically either omitted or classified as low density residential areas. Although low density may be a suitable classification for airports, which have few buildings, and a multitude of pervious and impervious surfaces, it does not characterize industrial complexes. The urban dataset requires further development to enhance coverage of these sparsely populated districts.

The urban spatial extent dataset has a resolution of 1km, which allows for a reasonable level of generalization considering the global scale of the project. Furthermore, this is the resolution of LandScan, so the same methods can be employed with future versions of LandScan. Given that the intended use of the dataset is to represent urban systems in GCM's with a grid resolution on the order of at least 100 km, this resolution is sufficient to represent the intended processes at the GCM scale. However, if the dataset were to be used for higher resolution studies, users must first consider if the dataset is accurate enough for meaningful representations of urban systems at smaller scales.

The same limitation exists for the building characteristics. Only three building types were noted for each regional category, which should reasonably describe the overall character of a place and, even more importantly, point out contrasting elements between regions. Again, the database is suitable for global level analysis, but it is unlikely to be appropriate at smaller scales. However, the dataset as developed here should not be considered a final product. Using this project as a starting point, it would be relatively easy to further segregate regions and to add information to the dataset as it becomes available. In that sense this dataset should be considered a living document that is intended to be added to over time and that should use wide ranging participation from other researchers to fill in or improve areas presently lacking in detail. The format of the database allows for progressive expansion of the data, and its design allows for scale modification to make it suitable for regional or local studies.

In summary, the extent dataset and building database should not be considered to be in their final form, as the continuous opportunity exists to add to and further improve them. These datasets should only be used for studies at an appropriate scale. For smaller-scale studies, the information presented here can be used as a guide to create databases with greater detail.

7. Future work

Future additions and improvements to the dataset

The urban spatial extent boundaries are defined by population density. As discussed in the previous section, urban landscapes where few people reside such as airports and industrial complexes are either categorized as low density residential or absent from the dataset altogether because of sparse population. A forthcoming dataset of urban extent produced by the MODIS landcover team (Schneider 2007) will be evaluated for its potential in filling in these "industrial" gaps.

Another way to add to and improve the urban extent database is to incorporate a temporal component. Population projections exist for the world going back several hundred years (*e.g.* McEvedy and Jones 1978). To complement this data, there are historical estimates of urban growth (*e.g.* Chandler 1987). Using this information, the urban extent database can be adapted to represent urban areas back in time. Moreover, we can project the growth of urban areas into the future with population projections.

Future urban extent datasets may improve as LandScan improves. LandScan is currently developing a dataset that illustrates where people are during a 24-hour period (Bright 2005). This information may help define tall building districts with greater accuracy, as many TBDs are used primarily for business-related purposes, so population density based on residency may not accurately locate them. In looking at daytime/nighttime differences, however, this LandScan dataset has shortcomings since its developers will not disclose their sources. Nondisclosure of methods and data sources is a serious problem, since any result from using the data would not be verifiable.

The database of building properties comprises nearly all the information needed to run the urban sub-model. Additional model requirements include percent roof area and percent pervious surface for each regional category. These parameters were not included in this thesis because they did not require the development of a specialized methodology.

The information for these parameters can be easily assembled using known methods and data. The Emporis database includes information on ground floor area for tall building districts and many high density areas throughout the world. This will be used in conjunction with residential building trade information to complete percent roof area estimates for each region and urban class. Pervious surfaces (often referred to as percent vegetation) for regional categories will be established based on category definitions. Definitions of urban intensity consider, as a major component, the amount of vegetation present. Therefore standardized relationships can be applied taking into consideration regional variations, and the resulting information can be applied globally to determine percent pervious surface.

NCAR GCM and other potential uses

Once CLM-Urban is validated (ongoing), the urban extent dataset and building properties database will be used in a GCM run. The model output will answer long-standing questions about how urban areas influence climate. NCAR and others can use this dataset to help answer pressing questions posed by international groups such as the Intergovernmental Panel on Climate Change (IPCC). Questions to be addressed include: Do urban areas influence global climate patterns? If urban heat islands to have an effect, to what extent do they influence climate and how? How can we change urban systems to mitigate negative influences on global climate? The initial model run seeks to answer these questions and will bring new questions to light.

Because prior to this thesis no global dataset of urban characteristics existed, the resulting datasets will be useful to the scientific community. Possible applications include improvement of the urban classification of land cover datasets and better inputs for meso-scale meteorological models. The final question posed above points out possibly the greatest potential for the dataset presented here. Studies of scenarios in which certain thermal or radiative properties are altered can tell us a great deal about how we might be able to mitigate the warming effect of urban areas. For instance, it would be useful to know how changing all roof types to be highly reflective would influence the urban heat island effect on a regional or global scale.

Alternatively, how would increasing impervious surfaces and covering all roofs with vegetation or solar cells change latent heat flux? Since a primary cause of urban heat islands is increased heat storage and decreased latent heat flux (Landsberg 1981), adjusting model parameters that address these fluxes can tell us how to affect change in urban climates.

Another relationship worth exploring is urban morphology parameters. As urban intensity increases (e.g. greater population density, taller buildings), the urban heat island also gains intensity (Terjung and O'Rourke 1980a). Will curbing urban sprawl by creating more densely built cities help or harm warming mitigation strategies?

In a related vein, by incorporating urban models in GCMs it is also possible to better assess the climate impacts within an urban area as compared to impacts on nearby rural areas. Finally, combining urban population statistics and urban climate impacts allows for better assessment of climate impacts on urban populations. This end result may help policymakers and stakeholders discover new ways to mitigate global warming.

8. References

Akbari, H. and A. Desjarlais. 2007. *Cooling Down the House – Residential roofing products soon will boast "cool" surfaces*. National Roofing Contractors Association. http://www.professionalroofing.net/article.aspx?A_ID=609.

Anandakumar, K. 1999. A study on the partition of net radiation into heat fluxes on a dry asphalt surface. *Atmospheric Environment* 33: 3911-3918.

Arnfield, A.J. 1982. Estimation of diffuse irradiance on sloping, obstructed surfaces: an error analysis. *Archives for Meteorology, Geophysics, and Bioclimatology B* 30: 303-320.

Arnfield, A.J. 1984. Simulating radiative energy budgets within the urban canopy layer. *Modeling and Simulation* 15: 227-233.

Arnfield, A.J. 2000. A simple model of urban canyon energy budget and its validation. *Physical Geography* 11: 220-239.

Arnfield, A.J.. 2003. Two decades of urban climate research: A review of turbulence, exchanges of energy and water, and the urban heat island. *International Journal of Climatology* 23: 1-26.

Arnfield, A.J. and C.S.B. Grimmond. 1998. An urban canyon energy budget model and its application to urban storage heat flux modeling. *Energy and Buildings* 27: 61-68.

Asaeda, T., V.T. Ca, and A. Wake. 1996. Heat storage of pavement and its effect on the lower atmosphere. *Atmospheric Environment* 30: 413-427.

Atkinson, B.W. 2003. Numerical modeling of urban heat-island intensity. *Boundary-Layer Meteorology* 109: 285-310.

Attoe, W., ed. 1988. *Transit, land use & urban form.* Austin, TX: The University of Texas at Austin.

Azaar, K., I.D. Rosco, and J.M. Vergnaud. 2002. Anisotropic swelling of thin EPDM rubber discs by absorption of toluene. *Polymer* 43: 4261-4267.

Baskaran, B.A., K.K.Y. Liu, W. Lei, and A.H. Delgado. 2003. A New facility to simulate simultaneous wind and thermal effects on roofing systems. *Journal of Testing and Evaluation* 31(4): 1-10. IRC pub no. NRCC-45672. http://irc.nrc-cnrc.gc.ca/pubs/fulltext/nrcc45672/

Becker, B.K. and C.A.G. Egler. 1992. *Brazil, a new regional power in the world-economy*. Cambridge: Cambridge University Press.

Berdahl, P. and S.E. Bretz. 1997. Preliminary Survey of the Solar Reflectance of Cool Roofing Materials. *Energy and Buildings* 25: 149-158.

Best, M.J. 2005. Representing urban areas within operational numerical weather prediction models. *Boundary-Layer Meteorology* 114: 91-109.

Best, M.J. 2006. Progress towards better weather forecasts for city dwellers: from short range to climate change. *Theoretical Applications in Climatology* 84: 47-55, doi:10.1007/s00704-005-0143-2.

Betts, R.A. 2001. Biogeophysical impacts of land use on present-day climate: near-surface temperature change and radiative forcing. *Atmos. Sci. Lett.* 2: doi:10.1006/asle.2001.0037.

Binici, H., Aksoganb, O, and T. Shah. 2005. Investigation of fibre reinforced mud brick as a building material. *Construction and Building Materials* 19(4): 313-318.

Bounoua, L., R. DeFries, G.J. Collatz, P. Sellers, and H. Khan. 2002. Effects of land cover conversion on surface climate. *Climate Change* 52: 29-64.
Bright, E. 2005. *Hold Still Waldo, We're Fixin' to Focus: LandScan Developments, Directions, and Applications.* Presented at The University of Kansas GIS Day Symposium, Nov. 16, 2005.
Brovkin, V., S. Sitch, W. von Bloh, M. Claussen, E. Bauer, and W. Cramer. 2004. Role of land cover changes for atmospheric CO_2 increase and climate change during the last 150 years. *Global Change Biology* 10: 1253-1266, doi:10.1111/j.1365-2486.2004.00812.x.
Brown, M. 2000. Urban parameterizations for mesoscale meteorological models. In *Mesoscale Atmospheric Dispersion*. ed. Z. Boybeyi, 193-255. Boston: WIT Press.
Brzev, S., Greene, M., and R. Sinha. 2007. *Rubble stone masonry walls with timber frame and timber roof.* In World Housing Encyclopedia, Housing Reports. Report ID 18, India. http://205.147.11.244/Report_Selection/list.asp?varCountry=India#ReportsList
Campbell, J.B. 2002. *Introduction to Remote Sensing*, 3rd ed. New York: The Guilford Press.
Carlson, T.N., J.K. Dodd, S.G. Benjamin, and J.N. Cooper. 1981. Satellite estimation of the surface energy balance, moisture availability and thermal inertia. *Journal of Applied Meteorology* 20:67-87.
Chandler, T. 198. *Four thousand years of urban growth: An historical consensus.* Lewiston, NY: Edwin Mellen Press.
Chapman, L., J.E. Thornes, and A.V. Bradley. 2001. Rapid determination of canyon geometry parameters for use in surface radiation budgets. *Theoretical and Applied Climatology* 69: 81-89.
CIESIN (Center for International Earth Science Information Network), Columbia University; International Food Policy Research Institute (IPFRI), the World Bank; and Centro Internacional de Agricultura Tropical (CIAT). 2004: Global Rural-Urban Mapping Project (GRUMP): Urban Extents. Palisades, NY: CIESIN, Columbia University. http://beta.sedac.ciesin.columbia.edu/gpw.
Cionco, R.M. and R. Ellefsen. 1998. High resolution urban morphology data for urban wind flow modeling. *Atmospheric Environment* 32: 7-17.
Clarke, D., ed. 1989. *Approaches to the study of traditional dwellings and settlements.* Berkeley, CA: Center for Environmental Design Research, University of California at Berkeley.
Clarke, J.A. 2001. *Energy Simulation in Building Design*, 2nd. ed. Oxford: Butterworth Heinemann.
Cleugh, H.A. and T.R. Oke. 1986. Suburban-rural energy balance comparisons in summer for Vancouver, B.C. *Boundary-Layer Meteorology* 36:351-369.
Copeland, J.H., R.A. Pielke, and T.G.F. Kittel. 1996. Potential climatic impacts of vegetation change: a regional modeling study. *Journal of Geophysical Research* 101: 7409-7418.
Cramer, W. and Coauthors. 2001. Global response of terrestrial ecosystem structure and function to CO_2 and climate change: results from six dynamic global vegetation models. *Global Change Biology* 7: 357-373.
DigitalGlobe. 2007. *FAQ.* http://www.digitalglobe.com/about/FAQ.shtml

Dobson, J. E., E. A. Bright, P.R. Coleman, R.C. Durfee, and B.A. Worley. 2000. LandScan: A Global Population Database for Estimating Populations at Risk. *Photogrammetric Engineering and Remote Sensing* 66 (7): 849-857.
Doll, D., J.K.S. Ching, and J. Kaneshiro. 1985. Parameterization of subsurface heating for soil and concrete using net radiation data. *Boundary-Layer Meteorology* 32: 351-372.
EarthSat. 2007. *MDA EarthSat Satellite Imagery.* http://www.earthsat.com/
Eastman, J.L., M.B. Coughenour, and R.A. Pielke, Sr. 2001. The regional effects of CO_2 and landscape change using a coupled plant and meteorological model. *Global Change Biology* 7: 797-815.
Ellefsen, R. 1990-91. Mapping and measuring buildings in the canopy boundary layer in ten U.S. cities. *Energy and Buildings* 15-16: 1025-1049.
Elvidge, C.D., P.C. Sutton, T.W. Wagner, R. Ryzner, J.E. Vogelmann, S.J. Goetz, A.J. Smith, C. Jantz, K.C. Seto, M.L. Imhoff, Y.Q. Wang, C. Milesi, and R. Nemani. 2004. Urbanization. In *Land Change Science: Observing, Monitoring and Understanding Trajectories of Change on the Earth's Surface*, ed. G. Gutman, A. C. Janetos, C.O. Justice, E.F. Moran, J.F. Mustard, R.R. Rindfuss, D. Skole, B.L. Turner II, and M.A Cochrane, 315-328. The Netherlands: Kluwer Academic Publishers.
Emporis Corporation. 2007. Emporis Buildings - The Building Industry Platform. http://www.emporis.com/en/ (accessed 3/07).
Feddema, J.J., K.W. Oleson, G. Bonan, L.O. Mearns, L.E. Buja, G.A. Meehl, and W.M. Washington. 2005. The importance of land cover change in simulating future climates. *Science* 310: 1674-1678.
Foamglas. 2005. *Insulation of timber, woodwool slab, and cellular concrete roofs, new build.* Pittsburgh Corning. www.foamglas.co.uk.
Foamglas. 2006. *Permaphalt Polymer Modified Asphalt for concrete, metal deck, timber, and woodool slab roofs.* Pittsburgh Corning. www.foamglas.co.uk.
Foamglas. 2007. *Insulation for concrete decks - new build or renovation*. http://www.foamglas.co.uk.
Foley, J.A., and Coauthors. 2005. Global consequences of land use. *Science* 309: 570-574.
Frank, R.S., R.B. Gerding, P.A. O'Rourke, and W.H. Terjung. 1981a. Simulating urban obstructions. *Simulation* 36: 83-92.
Frank, R.S., R.B. Gerding, P.A. O'Rourke, and W.H. Terjung. 1981b. An urban radiation obstruction model. *Boundary-Layer Meteorology* 20: 259-264.
Fronapfel, E. L., and B.J. Stolz. 2006. Emissivity Measurements of Common Construction Materials*. InfraMation 2006.* EI Professional Investigative Engineers, Inc.
Fu, C. 2003. Potential impacts of human-induced land cover change in East Asia monsoon. *Global Planet Change* 37: 219-229, doi:10.1016/S0921-8181(02)00207-2.
Givoni, B. 1976. *Man Climate and Architecture*. 2^{nd} ed. London: Applied Science Publishers.
Grimmond, C.S.B. 1992. The suburban energy balance: methodological considerations and results for a mid-latitude west coast city under winter and spring conditions. *International Journal of Climatology* 12:481-497.

Grimmond, C.S.B. 2007. Urbanization and global environmental change: local effects of urban warming. *The Geographical Journal.* 173: 83-88.
Grimmond, C.S.B., H.A. Cleugh, and T.R. Oke. 1991. An objective urban heat storage model and its comparison with other schemes. *Atmospheric Environment* 25B: 311-326.
Grimmond, C.S.B. and T.R. Oke. 1991. An evapotranspiration–interception model for urban areas. *Water Resources Research* 27: 1739–1755.
Grimmond, C.S.B., and T.R. Oke. 1995. Comparison of heat fluxes from summertime observations in the suburbs of four North American cities. *Journal of Applied Meteorology* 34:873-889.
Grimmond, C.S.B. and T.R. Oke. 1999. Heat storage in urban areas: Local-scale observations and evaluation of a simple model. *Journal of Applied Meteorology* 4(7): 922-940.
Grimmond, C.S.B and C. Souch. 1994. Surface description for urban climate studies: a GIS based methodology. *Geocarto International* 1: 47-59.
Grimmond, C.S.B., C. Souch, and M.D. Hubble. 1996. Influence of tree cover on summertime surface energy balance fluxes, San Gabriel Valley, Los Angeles. *Climate Research* 6:45-57.
Henry, J.A., and S.E. Dicks. 1987. Association of urban temperatures with land use and surface materials. *Landscape and Urban Planning* 14:21-29.
Henry, J.A., S.E. Dicks, and G.A. Marotz. 1985. Urban and rural humidity distributions: relationships to surface materials and land use. *Journal of Climatology* 5:53-62.
Houghton, R.A and coauthors. 1983. Changes in the carbon content of terrestrial biota and soils between 1860 and 1980: A net release of CO_2 to the atmosphere. *Ecological Monographs* 53:235-262.
Houghton, R.A., and J.L. Hackler. 1995. *Continental scale estimates of the biotic carbon flux from land cover change: 1850-1980*. ORNL/CDIAC-79, NDP-050, Carbon Dioxide Information Analysis Center, Oak Ridge National Laboratory, U.S. Department of Energy, Oak Ridge, Tennessee.
Houghton, R.A. 1999. The annual net flux of carbon to the atmosphere from changes in land use 1850-1990. *Tellus* 51B:298-313.
Houghton, R.A. and J.L. Hackler. 2001. *Carbon flux to the atmosphere from land-use changes: 1850 to 1990.* ORNL/CDIAC-79, NDP-050/R1, Carbon Dioxide Information Analysis Center, Oak Ridge National Laboratory, U.S. Department of Energy, Oak Ridge, Tennessee.
Houghton, R.A. 2002. Revised estimates of the annual net flux of carbon to the atmosphere from changes in land use and land management 1850-2000. *Tellus* 52.
Ichinose T., K. Shimodozono, and K. Hanaki. 1999. Impact of anthropogenic heat on urban climate in Tokyo. *Atmospheric Environment* 33: 3897–3909.
Infrared Services, Inc. 2007. Emissivity Values for Common Materials. http://infrared-thermography.com/material-1.htm
Intergovernmental Panel on Climate Change. 2006. About IPCC. http://www.ipcc.ch/about/about.htm.
Johnson, G.T. and I.D. Watson. 1984. The determination of view-factors in urban canyons. *Journal of Climate and Applied Meteorology* 23: 329-335.

Johnson, G.T. and I.D. Watson, 1985: Reply. *Journal of Climate and Applied Meteorology* 24: 386.
Kalanda, B.D., T.R. Oke, and D.L. Spittlehouse, D.L. 1980. Suburban energy balance estimates for Vancouver, B.C., using the Bowen ratio-energy balance approach. *Journal of Applied Meteorology* 19: 791-802.
Kidder, S.Q., and O.M. Essenwanger.1995. The effect of clouds and wind on the difference in nocturnal cooling rates between urban and rural areas. *Journal of Applied Meteorology* 34:2440-2448.
Kjelgren, R. and T. Montague. 1998. Urban tree transpiration over turf and asphalt surfaces. *Atmospheric Environment* 32: 35-41.
Knauf Insulation, Ltd. 2004a. *Solid masonry and curtain walls: Non-residential.* Mar. 2004. http://www.knaufinsulation.co.uk/output/litdownload.html
Knauf Insulation, Ltd. 2004b. *Pitched roofs - new build and upgrade: Residential*. v.2. Dec. 2004. http://www.knaufinsulation.co.uk/output/litdownload.html
Knauf Insulation, Ltd. 2005a. *Flat roofs: Non-residential.* v. 4. Jul. 2005. http://www.knaufinsulation.co.uk/output/litdownload.html
Knauf Insulation, Ltd. 2005b. *Pitched roofs: Non-residential.* v. 2. Aug. 2005. http://www.knaufinsulation.co.uk/output/litdownload.html
Landsberg, H.E. 1981. *The Urban Climate.* New York: Academic Press.
Lawrence-Berkeley National Laboratory. 2000. *Cool Roofing Materials Database.* http://eetd.lbl.gov/CoolRoofs/
Levinson, R. and A. Hashem. 2001. *Effects of Composition and Exposure on the Solar Reflectance of Portland Cement Concrete.* Lawrence Berkeley National Laboratory Pub. No. LBNL-48334-2001.
Liu, Y., F. Chen, T. Warner, S. Swerdlin, J. Bowers, and S. Halvorson. 2004. Improvements to surface flux computations in a non-local-mixing PBL scheme, and refinements to urban processes in the Noah land-surface model with the NCAR/ATEC real-time FDDA and forecast system. *20th Conference on Weather Analysis and Forecasting/16th Conference on Numerical Weather Prediction*. 11-15 January, 2004, Seattle, Washington.
Maref, W., M.M. Manning, M.A. Lacasse, M.K. Kumaran, S.M. Cornick, and M.C. Swinton. 2007. *Laboratory demonstration of solar driven inward vapour diffusion in a wall assembly*. 11th Canadian Conference on Building Science and Technology, Banff, Alberta: March 22, 2007. IRC Pub no. NRCC-49203. http://irc.nrc-cnrc.gc.ca/pubs/fulltext/nrcc49203/
Marsh, G.P. 1864. *Man and Nature*. Massachusetts: Harvard University Press.
Masson, V. 2000. A physically-based scheme for the urban energy budget in atmospheric models. *Boundary-Layer Meteorology* 94: 357-397.
Masson, V. 2006. Urban surface modeling and the meso-scale impact of cities. *Theoretical and Applied Climatology* 84, 35-45, doi:10.1007/s00704-005-0142-3.
Master Wall, Inc. 2006. *Light Reflectance of Finishes.* Technical Bulletin MW# 160-040106.
Mathews, H.D., A.J. Weaver, K.J. Meissner, N.P. Gillett, and M. Eby. 2004. Natural and anthropogenic climate change: incorporating historical land cover change, vegetation dynamics and the global carbon cycle. *Climate Dynamics* 22: 461-479, doi:10.1007/s00382-004-0392-2.
McEvedy, C. and R. Jones. 1978. A*tlas of World Population History.* New York:

Penguin.
Mills, G.M. 1993. Simulation of the energy budget of an urban canyon – I. Model structure and sensitivity test. *Atmospheric Environment B* 27: 157-170.
Mukhopadhyaya, P., Kumaran, K., Tariku, F. and D. van Reenen. 2003. *FINAL REPORT FROM TASK 7 OF MEWS PROJECT AT THE INSTITUTE FOR RESEARCH IN CONSTRUCTION - Long-Term Performance Predict the Moisture Management Performance of Wall Systems as a Function of Climate, Material Properties, etc. Through Mathematical Modelling*. National Resource Council of Canada Pub. No. IRC-RR-132.
Mukhopadhyaya, P., M.K. Kumaran, and D. van Reenen. 2004a. *Vapour barrier and moisture response of wood-frame stucco wall - results from hygrothermal simulation*. CIB World Building Congress 2004, Toronto, Ontario: May 02, 2004. IRC pub no. NRCC-46864. http://irc.nrc-cnrc.gc.ca/pubs/fulltext/nrcc46864/
Mukhopadhyaya, P., M.K. Kumaran, D. van Reenen, and F. Tariku. 2004b. *Application of modeling tool to assess moisture and thermal performance of retrofitted wall assemblies.* CIB World Building Congress 2004, Toronto, Ontario: May 02, 2004. IRC Pub no. NRCC-46869. http://irc.nrc-cnrc.gc.ca/pubs/fulltext/nrcc46869/
Myhre, G., and A. Myhre. 2003. Uncertainties in radiative forcing due to surface albedo changes caused by land-use changes. *Journal of Climate* 16: 1511-1524.
Narisma, G.T. and A.J. Pitman. 2003. The impact of 2000 years of land cover change on the Australian near-surface climate. *Journal of Hydrometeorology* 4: 424-436.
National Aeronautics and Space Administration (NASA). 2005. NASA news feature, *Tropical Deforestation Affects Rainfall in the U.S. and Around the Globe*. www.nasa.gov/centers/goddard/news/topstory/2005/deforest_rainfall.html
National Association of Home Builders. 2003. *Consumer Practices Report, 2002 Product Usage*. NAHB Research Center, Inc.
National Resources Canada (NRC). 2006. RADARSAT-1 Overview. http://ccrs.nrcan.gc.ca/radar/spaceborne/radarsat1/specs/index_e.php#Top
Nichol, J.E. 1996. High-resolution surface temperature patterns related to urban morphology in a tropical city: a satellite-based study. *Journal of Applied Meteorology* 35:135-146.
Oak Ridge National Laboratories. 2005. *LandScan 2004 Global Population*. Published by UT Battelle.
Oke, T. R. 1974. *Review of urban climatology, 1968-1973*. Technical Note 134 (publication No. 383). Geneva: World Meteorological Organization.
Oke, T.R. 1979. *Review of Urban Climatology, 1973-1976.* Technical Note 169 (publication No. 539). Geneva: World Meteorological Organization.
Oke, T.R. 1982. The energetic basis of the urban heat island. *Quarterly Journal of the Royal Meteorology Society* 108: 1-24.
Oke, T.R. 1987. *Boundary Layer Climates*. 2nd ed. New York: Methuen & Co.
Oke, T.R. 1988. The urban energy balance. *Progress in Physical Geography* 12: 471-508.
Oke, T.R. 1989. The micrometeorology of the urban forest. *Philosophical Transactions of the Royal Society of London, Series B* 324: 335-349.

Oke, T.R. 1995: The heat island characteristics of the urban boundary layer: Characteristics, causes and effects. In *Wind Climate in Cities*, eds. J.E. Cermak, A.G. Davenport, E.J. Plate, and D.X. Viegas, 81–107. Netherlands: Kluwer Academic.
Oke, T.R. and H.A. Cleugh. 1987. Urban heat storage derived as energy balance residuals. *Boundary-Layer Meteorology* 39:233-245.
Oke, T.R., G.T. Johnson, D.G. Steyn, and I.D. Watson. 1991. Simulation of surface urban heat islands under "ideal" conditions at night, part 2: diagnosis of causation. *Boundary-Layer Meteorology* 56: 339-358.
Oke, T.R. and J.H. McCaughey. 1983. Suburban-rural energy balance comparisons for Vancouver, B.C.: an extreme case? *Boundary-Layer Meteorology* 26:337-354.
Oke, T.R., R.A. Spronken-Smith, E. Jáuregui, and C.S.B. Grimmond. 1999. The energy balance of central Mexico City during the dry season. *Atmospheric. Environment* 33: 3919-3930.
Oleson, K.W., Y. Dai *et al.* 2004. *Technical description of the Community Land Model (CLM)*, NCAR Technical Note NCAR/TN-461+STR.
Oleson, K., G. Bonan, and J. Feddema. 2006. Development of an urban parameterization for a global climate model. Presentation for the American Meteorological Society annual meeting, 2006.
Oleson, K.W., G.B. Bonan, J. Feddema, M. Vertenstein, and C.S.B. Grimmond. 2007a. An urban parameterization for a global climate model: 1. Formulation and evaluation for two cities. *Forthcoming, Journal of Applied Meteorology and Climatology.*
Oleson, K.W., G.B. Bonan, J. Feddema, M. Vertenstein, and C.S.B. Grimmond. 2007b. An urban parameterization for a global climate model: 2. Sensitivity to input parameters and the simulated urban heat island in offline simulations. *Forthcoming, Journal of Applied Meteorology and Climatology.*
Olgyay, V. 1992. *Design with Climate.* New York: Van Nostrand Reinhold.
Omega Engineering, Inc. 2007. Emissivity of common materials. http://www.omega.com/literature/transactions/volume1/emissivity.html
Paroli, R.M., O. Dutt, and C. Frégeau. 1996. *Properties and performance of roof coverings.* Building Better Roofs: IRC Technical Seminar, pp. 1-30, December 01, 1996 (Reprinted in: Building Better Roofs: IRC Technical Seminar (NRCC-40627)). http://irc.nrc-cnrc.gc.ca/pubs/fulltext/nrcc40627-7/
Paterson, D.A. and C.J. Apelt. 1989. Simulation of wind flow around three-dimensional buildings. *Building and Environment* 24: 39-50.
Pielke, R.A., Sr., G. Marland, R.A. Betts, T.N. Chase, J.L. Eastman, J.O. Niles, D.D.S. Niyogi, and S.W. Running. 2002. The influence of land-use change and landscape dynamics on the climate system: relevance to climate-change policy beyond the radiative effect of greenhouse gases. *Philosophical Transactions of the Royal Society of London A* 360: 1705-1719.
Portland Cement Association (PCA). 2007. *What is the correct thickness of stucco?* www.cement.org/stucco/faq_thickness.asp
Premier Steel Building, Inc. (PSBI). 2007*. What makes our builldings the best in the industry?* http://www.premiersteel.org/Specifications.htm
Quattrochi, D.A. and Q. Weng. 2006. *Urban Remote Sensing.* CRC Press.

Reagan, J.A. and D.M. Acklam. 1979. *Energy and Buildings* 2: 237-248.
Roofhelp.com. 2007. *EPDM Rubber.* www.roofhelp.com/choices/epdm/
Roth, M. and T.R. Oke. 1995. Relative efficiencies of turbulent transfer of heat, mass, and momentum over a patchy urban surface. *Journal of the Atmospheric Sciences* 52:1863-1874.
Roth, M., T.R. Oke, and W.J. Emery. 1989. Satellite-derived urban heat islands from three coastal cities and the utilization of such data in urban climatology. *International Journal of Remote Sensing* 10:1699-1720.
Sahal, N. and M.A. Lacasse. 2004. *Experimental Assessment of Water Penetration and Entry into Siding-Clad Wall Specimen. Internal Report, Institute for Research in Construction, National Research Council Canada,* IRC-IR-862. http://irc.nrc-cnrc.gc.ca/pubs/ir/ir862/
Sailor, D.J., and L. Lu. 2004. A top-down methodology for developing diurnal and seasonal anthropogenic heating profiles for urban areas. *Atmospheric Environment* 38: 2737-2748.
Scheffler, M.J. 2007. Thin stone wall systems. *Whole Building Design Guide.* National Institute of Building Sciences. www.wbdg.org/design/env_wall_thin_stone.php
Schmid, H.P., H.A. Cleugh, C.S.B. Grimmond, and T.R. Oke. 1991. Spatial variability of energy fluxes in suburban terrain. *Boundary-Layer Meteorology* 54: 249–276.
Schmugge, T.J., J.R. Wang, and G. Asrar. 1988. Results from the Push Broom Microwave Radiometer flights over the Konza Prairie in 1985*. IEEE Transactions on Geoscience and Remote Sensing* 26 (5):590-96.
Schneider, A. 2007. *Mapping global urban extent, intensity and vegetation using the fusion of MODIS satellite imagery and ancillary data sources.* Presented at the Association of American Geographers annual meeting, April 4, 2007.
Schneider, A., M.A. Friedl, D.M. McIver, and C. E. Woodcock. 2003. Mapping Urban Areas by Fusing Multiple Sources of Coarse Resolution Remotely Sensed Data. *Photogrammetric Engineering and Remote Sensing* 69(12): 1377-1386.
Schwartz, T.A. 2001. Glass and metal curtain-wall fundamentals. *APT Bulletin* 32(1): 37-45.
Sellers, P.J., and coauthors. 1997. Modeling the exchanges of energy, water, and carbon between continents and the atmosphere. *Science* 275: 502-509.
Shepherd, J.M. 2005. A review of current investigations of urban-induced rainfall and recommendations for the future. *Earth Interactions* 9: 1-27.
Sitch, S., B. Smith, I.C. Prentice, A. Arneth, A. Bondeau, W. Cramer, J.O. Kaplan, S. Levis, W. Lucht, M.T. Sykes, K. Thonicke, and S. Venevsky. 2003. Evaluation of ecosystem dynamics, plant geography and terrestrial carbon cycling in the LPJ dynamic global vegetation model. *Global Change Biology* 9: 161-185.
Steyn, D.G. 1980. The calculation of view factors from fisheye-lens photographs. *Atmosphere-Ocean* 18: 254-258.
Steyn, D.G. and T.J. Lyons. 1985. Comments on “The determination of view-factors in urban canyons”. *Journal of Climate and Applied Meteorology* 24: 383-385.
Steyn, D.G., J.E. Hay, I.D. Watson, and G.T. Johnson. 1986. The determination of sky view-factors in urban environments using video imagery. *Journal of Atmospheric and Oceanic Technology* 3: 759-764.

Stohlgren, T.J., T.N. Chase, R.A. Pielke, Sr., T.G.F. Kittel, and J.S. Baron. 1998. Evidence that local land use practices influence regional climate, vegetation, and stream flow patterns in adjacent natural areas. *Global Change Biology* 4: 495-504.
Straube, J.F. and E.F.P Burnett. 2005. *Building Science for Building Enclosures.* Westford: Building Science Press, Inc.
Suckling, P.W. 1980. The energy balance microclimate of a suburban lawn. *Journal of Applied Meteorology* 19: 606-608.
Taha, H., D. Sailor, and H. Akbari. 1992. *High Albedo Materials for Reducing Energy Building Cooling Energy Use*. Lawrence Berkeley National Laboratory Pub. No. LBL-31721.
Taha, H. 1999. Modifying a mesoscale meteorological model to better incorporate urban heat storage: a bulk-parameterization approach. *Journal of Applied Meteorology* 38: 466-473.
Terjung, W.H. and P.A. O'Rourke. 1980a. Simulating the causal elements of urban heat islands. *Boundary-Layer Meteorology* 19: 93-118.
Terjung, W.H. and P.A. O'Rourke. 1980b. Influences of physical structures on urban energy budgets. *Boundary-Layer Meteorology* 19: 421-439.
Thatch.org. 2007 *Thatch roof and materials specification. http://thatch.org/spec.htm*
Thomas, Jr., W. L., ed. 1956. *Man's Role in Changing the Face of the Earth*. Chicago: The University of Chicago Press.
Turner II, B.L. , W. C. Clark, R. W. Kates, J. F. Richards, J. T. Mathews, and W. B. Meyer, eds. 1990. *The earth as transformed by human action. Global and regional changes in the biosphere over the past 300 years*. Cambridge: Cambridge University Press with Clark University.
United States Army Corps of Engineers (USACE). 1998. Technical Instructions: Structural Considerations for Metal Roofing. TI 809-29, Engineering Instructions no. 015908. http://www.hnd.usace.army.mil/techinfo/ti/809-29.pdf.
Verseghy, D.L. and D.S. Munro. 1989a. Sensitivity studies on the calculation of the radiation balance of urban surfaces: I. Shortwave radiation. *Boundary-Layer Meteorology* 46: 309-331.
Verseghy, D.L. and D.S. Munro. 1989b. Sensitivity studies on the calculation of the radiation balance of urban surfaces: II. Longwave radiation. *Boundary-Layer Meteorology* 46: 309-331.
Vigener, N. and M.A. Brown. 2007. Curtain walls. *Whole Building Design Guide.* National Institute of Building Sciences. www.wbdg.org/design/env_fenestration_cw.php
Viterito, A. 1989. Changing thermal topography of the Baltimore-Washington corridor: 1950-1979. *Climatic Change* 14:89-102.
Voogt, J.A., and C.S.B. Grimmond. 2000. Modeling surface sensible heat flux using surface radiative temperatures in a simple urban area. *Journal of Applied Meteorology* 39: 1679-1699.
Vukovich, F.M. 1983. An analysis of the ground temperature and reflectivity pattern about St. Louis, Missouri, using HCMM satellite data. *Journal of Climate and Applied Meteorology* 22: 560-571.

Wang, H., A.J. Pitman, M. Zhao, and R. Leemans. 2003. The impact of land-cover modification on the June meteorology of China since 1700, simulated using a regional climate model. *International Journal of Climatology* 23: 511-527.
Watson, I.D. and G.T. Johnson. 1987. Graphical estimation of sky view-factors in urban environments. *Journal of Climatology* 7: 193-197.
Weast, R. C., ed. 1981. *Handbook of Chemistry and Physics, 61st ed*. Boca Raton, FL: CRC Press, p. E-398.
Wechsler, A.E. and P.E. Glaser. 1966. *Surface Characteristic Effect on Thermal Regime: Phase I.* Special Report (88), U.S. Army, Cold Regions Research and Engineering Lab, Hanover, New Hampshire.
Yap, D. and T.R. Oke. 1974. Sensible heat fluxes over an urban area – Vancouver, B.C. *Journal of Applied Meteorology* 13:880-890.

9. Appendices

Appendix A – Validation cities by region

Alaska	Australia	Brazil	Canada	Carribean
Anchorage	Sydney	Sao Paulo	Montreal	Havana
Kotzebne	Melbourne	Taboao de Serra	Ottawa	Kingston
Fairbanks	Bendings	Jandira/Itapevi	Saskatoon	Port au Prince
Kodiak	Wagga Wagga	Barueri	Calgary	San Juan
Prudhoe Bay	Newcastle	Jundiai	Edmonton	Santiago
Barrow	Canberra	Atibaia	Vancouver	Santo Domingo
Juneau	Mackay	Rio de Janeiro	Victoria	Holguin
Sitka	Townsville	Mesquita	Toronto	Santa Clara
Cordova	Perth	Belem	Sidney	Port of Spain
Ketchikan	Rockingham	Curitiba	Quebec	Castries
	Darwin	Jpessoa		
	Bagot	Manaus		
		Porto Alegre		
		Salvador		
		Santos		

China	C_Africa	C_Asia	E_Asia	E_Africa
Shanghai	Kinshasa	Almati	Pyongyang	Lagos
Suzhou	Brazzaville	Ulaanbaatar	Nampo	Ikorodu
Jiazing	Luanda	Baki/Baku	Songnim	Kano
Fuzhou	Mbuji-Mayi	Bakixanov	Seoul	Kaduna
Nantong	Bafoussam	Sumqayit	Suwon	Ibadan
Kashi	Bamenda	Tashkent	Gunpo	Benin
Lasa	Douala	Angren	Uiwang	Adis Ababa
Chongqing	Malabo	Baku	Anyang	Antananarivo
Xi'an	Uvira	T'Bilisi	Bucheon	Dodoma
Xianyang	Lubumbashi	Dushanbe	Kimpo	Kampala
Beijing	N'Djamena	Karaganda	Tokyo	Kigali
Canton		Bishkek	Hiratsuka	Maputo
Chengdu		Ashgabat	Minamiashigara	Nairobi
Haikou		Astana	Odawara	Bujumbura
Tianjin		Yerevan	Sendai	Mogadishu
Shenyang			Yamagata	Lusaka
			Taipei	Djibouti
			Hamamatsu	Lilongwe
			Nagoya	
			Naha	
			Osaka	
			Kyoto	
			Sapporo	

Appendix A, continued

E_Europe	Greenland	India	Mid_Amer	Mid_East
Warsaw	Nuuk	Hyderabad	Mexico City	Riyadh
Wroclaw	Maniitsoq	Indore	Tlalnepantla	Lefkosia
Poznan	Tasiilaq	Mumbai	Ojo de Aqua	Istanbul
Bydgoszcz	Ittoqqortoormiit	Thana	Toluca	Sultanbeyli
Grudziadz	Sisimint	Navi Mumbai	San Jose	Ankara
Torun	Kangerlussauq	Utan	Panama City	Baghdad
Gdynia	Illulissat	Ulhasnagar/Kalyan	San Miguelito	Tehran
Gdansk	Uummannaq	Bhiwandi	La Chorrera	Eslamshahr
Bucharest	Qeqertarsuaq	Dehli	San Salvador	al Basrah
Kiev	Qaqortoq	Bangalore	Managua	Hawalli
Minsk		Bombay	Guatemala City	Abu Dhabi
Prague		New Delhi	Monterrey	Doha
Riga		Calcutta	Pachuca	Kuwait City
Sarajevo		Madras	Guadalajara	Muscat
Herzegovina		Ahmadabad	Belmopan	Sana'a
Vilnius		Gauhati		al Manamah
Tallinn		Ernakulam		Beirut
Chisinau		Nagpur		

N_Africa	N_Europe	NC_US	NE_US	NW_US
Alexandria	Stockholm	Chicago	New York City	Seattle
Algiers	Oslo	Minneapolis	Baltimore	Portland
Asmara	Copenhagen	Pierre	Philadelphia	Tacoma
Cairo	Bergen	Bismarck	Detroit	Beaverton
Casablanca	Helsinki	Madison	Akron	Boise
Khartoum	Birmingham	Des Moines	Rochester	Cheyenne
Nouakchott	Cardiff	Sioux City	Buffalo	Laramie
Tripoli	Dublin	Lincoln	Cleveland	Great Falls
Tunis	London	Champaign	Boston	Spokane
Tangier	Edinburgh	Fargo	Washington D.C.	Opportunity
		Rapid City		

Appendix A, continued

Oceania	**Russia**	**S_Africa**	**S_Asia**	**S_Europe**
Honiara	Moscow	Nelspruit	Dhaka	Athens
Moresby	Vidnoje	Maseru	Tungi	Barcelona
Taytay	St. Petersburg	Cape Town	Narsingdi	Las Palmas
Saipan	Murmansk	Pretoria	Khulna	Lisbon
Koror	Arcangel	Mbabane	Chatlagam	Madrid
Hagatna	Rostov-na-donu	Harere	Barisal	Milan
Bairiki	Chelyabinsk	Johannesburg	Sandip	Naples
Honolulu	Norilsk	Windhoek	Colombo	Thessaloniki
Papeete	Novosibirsk	Durban	Kathmandu	Rome
Apia	Vladivostok	Bloemfontein	Lalitpur	Valletta
Pago Pago	Khabarovsk	Gaborone	Thimpu	
		Chittagong		
		Islamabad		
		Kabul		
		Karachi		
		Lahore		
		Heart		
		Uleguma		
		Male		

SC_US	**SE_Asia**	**SE_US**	**SW_US**	**Temp_SAm**
Austin	Rangoon	Atlanta	Los Angeles	Buenos Aires
Houston	Singapore	Miami	Malibu	La Plata
Dallas	Johor Baharu	Charlotte	Oxnard	Cordoba
San Antonio	Padang	Pensacola	San Diego	Santiago
St. Louis	Medan	New Orleans	Phoenix	Asuncion
Kansas City	Manila	Richmond	Albuquerque	Mendoza
Wichita	Taytay	Memphis	Denver	Bahia Blanca
Tulsa	Cibu	Louisville	Las Vegas	Montevideo
Oklahoma City	village	Birmingham	San Francisco	La Paz, Uruguay
El Paso	Ho Chi Minh City	Orlando	Oakland	Mar del Plata

Appendix A, continued

Trop_SAm	W_Africa	W_Eur
Lima	Lagos, nigeria	Berlin
Callao	Abidjan	Paris
Maracaibo	Ikorodu	Vienna
Caracas	Lome	Linz
Medellin	Bouake	Leipzig
Itagui	Treichville	Amsterdam
Barranquilla	Kumasi	Lichtenstein
San Cristobal, ven	Yamoussoukro	Oelsnitz
Cucuta	Conakry	Marseille
Quito	Dakar, Senegal	Brussels

Appendix B – Wall and roof types and frequency by regional category

Region	Cat	Ht(m)	H/W	Wall1	Roof1	%	Wall2	Roof2	%	Wall3	Roof3	%
Alaska	TBD	40	1.6	Conc panels/conc m	BUR/concrete deck	70	Brick veneer/conc m	BUR/concrete deck	20	Conc panels/conc m	Galv steel/metal bar	10
	HD	20	0.8	Conc panels/conc m	BUR/concrete deck	50	Brick veneer/conc m	BUR/concrete deck	40	Stone curtain/conc n	Shingles/wood deck	10
	LD	8	0.4	Wood frame/vinyl or	Shingles/wood deck	80	Wood frame/hardbr	Metal tiles	10	Wood frame/stucco	Ceramic tiles/wood c	10
Australia	TBD	200	8.0	Conc panels/conc m	BUR/concrete deck	60	Stone curtain/conc n	EPDM/steel deck	30	Glass curtain	Galv steel/metal bar	10
	HD	50	2.0	Brick veneer/conc m	Ceramic tiles/wood c	60	EIFS façade/wood fr	Metal tiles	20	Stone curtain/conc n	PVC/steel deck	20
	LD	8	0.4	Brick masonry, reinf	Ceramic tiles/wood c	40	Stone	Shingles/wood deck	30	Wood frame/vinyl or	Metal tiles	30
Brazil	TBD	120	4.8	Conc panels/conc m	BUR/concrete deck	70	Glass curtain	PVC/steel deck	20	Conc panels/conc m	EPDM/steel deck	10
	HD	40	1.6	Conc panels/conc m	BUR/concrete deck	60	Plaster veneer/brick	BUR/concrete deck	30	Brick masonry, reinf	Ceramic tiles/wood c	10
	LD	8	0.8	Wood frame/stucco	Ceramic tiles/wood c	60	Brick masonry, reinf	Corrugated metal (ir	20	wood frame	Corrugated metal (ir	20
C_Africa	TBD	70	2.8	Conc panels/conc m	Ceramic tiles/wood c	60	Conc panels/conc m	BUR/concrete deck	40			
	HD	20	0.8	Conc panels/conc m	Ceramic tiles/wood c	50	Concrete blocks	Corrugated metal (ir	40	Wood frame/unins w	Corrugated metal (ir	10
	LD	3	0.3	Concrete blocks	Corrugated metal (ir	50	Concrete blocks	Thatch	40	Wood frame/unins w	Thatch	10
C_Asia	TBD	60	2.4	Plaster veneer/brick	Galv steel/metal bar	50	Conc panels/conc m	PVC/steel deck	40	Glass curtain	BUR/concrete deck	10
	HD	30	1.2	Plaster veneer/conc	Galv steel/metal bar	70	Stone	Ceramic tiles/wood c	30			
	LD	8	0.8	Brick masonry, reinf	Ceramic tiles/wood c	50	Rubble	Corrugated metal (ir	30	Stone	Ceramic tiles/wood c	20
Canada	TBD	100	4.0	Conc panels/conc m	BUR/concrete deck	60	Glass curtain	Galv steel/metal bar	20	Brick veneer/conc m	Galv steel/metal bar	20
	HD	40	1.6	Conc panels/conc m	BUR/concrete deck	50	Brick veneer/conc m	Galv steel/metal bar	30	EIFS façade/wood fr	Metal tiles	20
	LD	8	0.4	Wood frame/hardbr	Shingles/wood deck	50	Brick masonry, reinf	Metal tiles	30	Wood frame/vinyl or	Shingles/wood deck	20
Caribbean	TBD	50	2.0	Conc panels/conc m	BUR/concrete deck	70	Plaster veneer/brick	Ceramic tiles/wood c	20	Glass curtain	EPDM/steel deck	10
	HD	20	0.8	Plaster veneer/brick	BUR/wood deck	50	Plaster veneer/conc	Ceramic tiles/wood c	40	Concrete blocks	Ceramic tiles/wood c	10
	LD	3	0.3	Brick masonry, reinf	Corrugated metal (ir	60	Wood frame/unins w	Ceramic tiles/wood c	30	Mud or adobe	Thatch	10
China	TBD	180	7.2	Conc panels/conc m	BUR/concrete deck	60	Glass curtain	EPDM/steel deck	20	Conc panels/conc m	Galv steel/metal bar	20
	HD	50	2.0	Brick veneer/conc m	BUR/wood deck	70	Conc panels/conc m	Ceramic tiles/wood c	30			
	LD	8	0.8	Brick masonry, reinf	Ceramic tiles/wood c	40	Mud or adobe	Corrugated metal (ir	40	Wood frame/wood s	Slate tiles	20
E_Africa	TBD	60	2.4	Conc panels/conc m	BUR/concrete deck	90	Stone curtain/conc n	Galv steel/metal bar	10			
	HD	20	0.8	Conc panels/conc m	BUR/wood deck	60	Concrete blocks	BUR/wood deck	40			
	LD	3	0.3	Concrete blocks	corrugated metal	50	Wood frame/unins w	Thatch	30	Corrugated metal	Corrugated metal (ir	20
E_Asia	TBD	180	7.2	Conc panels/conc m	BUR/concrete deck	50	Glass curtain	Galv steel/metal bar	30	Conc panels/conc m	EPDM/steel deck	20
	HD	50	2.0	Conc panels/conc m	BUR/concrete deck	50	Brick veneer/conc m	Galv steel/metal bar	40	EIFS façade/wood fr	Slate tiles	10
	LD	8	0.8	Wood frame/stucco	Ceramic tiles/wood c	40	Brick masonry, reinf	Slate tiles	40	Wood frame/wood s	Wood	20
E_Europe	TBD	90	3.6	Conc panels/conc m	BUR/concrete deck	80	Brick veneer/conc m	Galv steel/metal bar	10	Glass curtain	Galv steel/metal bar	10
	HD	40	1.6	Conc panels/conc m	Ceramic tiles/wood c	60	Brick veneer/conc m	Galv steel/metal bar	20	Stone	Ceramic tiles/wood c	20
	LD	8	0.8	Brick masonry, reinf	Ceramic tiles/wood c	50	Concrete blocks	Ceramic tiles/wood c	30	Concrete blocks	Corrugated metal (ir	20

Region	Cat	Ht(m)	H/W	Wall1	Roof1	%	Wall2	Roof2	%	Wall3	Roof3	%
Greenland	TBD	0	0.0	Conc panels/conc m	Galv steel/metal bar	50	Stone curtain/conc n	Galv steel/metal bar	50			
	HD	8	1.0	Conc panels/conc m	BUR/concrete deck	50	Galvanized steel	Galv steel/metal bar	50			
	LD	8	0.5	Wood frame/wood s	Shingles/wood deck	50	Galvanized steel	Metal tiles	30	Wood frame/vinyl or	Shingles/wood deck	20
India	TBD	80	3.2	Conc panels/conc m	BUR/concrete deck	80	Conc panels/conc m	PVC/steel deck	10	Brick masonry, reinf	BUR/concrete deck	10
	HD	30	1.2	Conc panels/conc m	BUR/concrete deck	50	Brick masonry, reinf	Ceramic tiles/wood c	30	Brick masonry, reinf	corrugated metal	20
	LD	3	0.3	Rubble	Corrugated metal (ir	60	Mud or adobe	Thatch	20	Wood frame/unins w	Corrugated metal (ir	20
Middle_Am	TBD	90	3.6	Conc panels/conc m	Ceramic tiles/wood c	50	Brick veneer/conc m	BUR/concrete deck	40	Glass curtain	steel	10
	HD	40	1.6	Conc panels/conc m	Ceramic tiles/wood c	50	Brick masonry, reinf	Corrugated metal (ir	40	Brick veneer/conc m	BUR/concrete deck	10
	LD	3	0.3	Brick masonry, reinf	Ceramic tiles/wood c	50	Wood frame/unins w	Corrugated metal (ir	30	Wood frame/stucco	Thatch	20
Mid_East	TBD	200	8.0	Conc panels/conc m	BUR/concrete deck	80	Glass curtain	EPDM/steel deck	20			
	HD	50	2.0	Conc panels/conc m	BUR/concrete deck	70	Brick masonry, reinf	BUR/concrete deck	30			
	LD	8	0.8	Concrete blocks	Ceramic tiles/wood c	50	Brick masonry, reinf	Ceramic tiles/wood c	30	Mud or adobe	Mud	20
N_Africa	TBD	80	3.2	Stone curtain/conc n	BUR/concrete deck	50	Conc panels/conc m	Ceramic tiles/wood c	40	Glass curtain	Galv steel/metal bar	10
	HD	30	1.2	Stone curtain/conc n	Ceramic tiles/wood c	60	Brick veneer/conc m	Mud	20	Mud or adobe	Metal tiles	20
	LD	8	0.8	Mud or adobe	Mud	40	Mud or adobe	Corrugated metal (ir	40	Brick masonry, reinf	Ceramic tiles/wood c	20
NC_US	TBD	120	4.8	Conc panels/conc m	BUR/concrete deck	60	Glass curtain	EPDM/steel deck	20	Stone curtain/conc n	Galv steel/metal bar	20
	HD	40	1.6	Conc panels/conc m	BUR/concrete deck	50	Brick veneer/conc m	Galv steel/metal bar	30	EIFS façade/wood fr	EPDM/steel deck	20
	LD	8	0.4	Wood frame/wood s	Shingles/wood deck	50	Wood frame/vinyl or	Ceramic tiles/wood c	30	Stone	Metal tiles	20
NE_US	TBD	160	6.4	Conc panels/conc m	BUR/concrete deck	60	Glass curtain	Galv steel/metal bar	30	Brick veneer/conc m	EPDM/steel deck	10
	HD	50	2.0	Conc panels/conc m	BUR/concrete deck	50	Brick veneer/conc m	Galv steel/metal bar	40	EIFS façade/wood fr	PVC/steel deck	10
	LD	12	0.6	Wood frame/wood s	Shingles/wood deck	40	Brick masonry, reinf	Ceramic tiles/wood c	30	Wood frame/vinyl or	Shingles/wood deck	30
N_Europe	TBD	100	4.0	Conc panels/conc m	Galv steel/metal bar	60	Glass curtain	Galv steel/metal bar	20	Stone curtain/conc n	BUR/concrete deck	20
	HD	40	1.6	Brick veneer/conc m	Ceramic tiles/wood c	50	Conc panels/conc m	Galv steel/metal bar	30	Galvanized steel	Galv steel/metal bar	20
	LD	12	1.2	Wood frame/hardbrc	Shingles/wood deck	50	Galvanized steel	Galv steel/metal bar	40	Wood frame/vinyl or	Metal tiles	10
NW_US	TBD	70	2.8	Conc panels/conc m	BUR/concrete deck	60	Glass curtain	Galv steel/metal bar	30	Brick veneer/conc m	BUR/wood deck	10
	HD	30	1.2	Conc panels/conc m	BUR/concrete deck	50	Brick veneer/conc m	Galv steel/metal bar	30	EIFS façade/wood fr	Ceramic tiles/wood c	20
	LD	8	0.4	Wood frame/vinyl or	Shingles/wood deck	40	Wood frame/wood s	Ceramic tiles/wood c	30	Brick masonry, reinf	Metal tiles	30
Oceania	TBD	100	4.0	Conc panels/conc m	BUR/concrete deck	90	Glass curtain	Galv steel/metal bar	10			
	HD	40	1.6	Conc panels/conc m	BUR/concrete deck	60	Concrete blocks	Shingles/wood deck	20	Corrugated metal	Corrugated metal (ir	20
	LD	8	0.8	Wood frame/unins w	Shingles/wood deck	50	Corrugated metal	Corrugated metal (ir	40	Wood frame/wood s	Shingles/wood deck	10
Russia	TBD	200	8.0	Conc panels/conc m	BUR/concrete deck	80	Conc panels/conc m	Galv steel/metal bar	20			
	HD	50	2.0	Conc panels/conc m	BUR/wood deck	70	Stone curtain/conc n	Galv steel/metal bar	20	Cement board/wood	BUR/wood deck	10
	LD	12	1.2	Brick masonry, reinf	Galv steel/metal bar	50	Wood frame/wood s	Shingles/wood deck	40	Stone	Metal tiles	10

Region	Cat	Ht(m)	H/W	Wall1	Roof1	%	Wall2	Roof2	%	Wall3	Roof3	%
S_Africa	TBD	80	3.2	Conc panels/conc m	BUR/concrete deck	70	Brick veneer/conc m	EPDM/steel deck	20	Glass curtain	Galv steel/metal bar	10
	HD	40	1.6	Conc panels/conc m	BUR/concrete deck	50	Cement board/wood	PVC/steel deck	30	Brick masonry, reinf	Corrugated metal (ir	20
	LD	8	0.8	Mud or adobe	Corrugated metal (ir	60	Corrugated metal	Corrugated metal (ir	20	Concrete blocks	Ceramic tiles/wood c	20
S_Asia	TBD	70	2.8	Conc panels/conc m	BUR/concrete deck	90	Glass curtain	Galv steel/metal bar	10			
	HD	30	1.2	Conc panels/conc m	BUR/wood deck	60	Mud or adobe	Mud	30	Galvanized steel	Corrugated metal (ir	10
	LD	3	0.3	Mud or adobe	Mud	70	Concrete blocks	Corrugated metal (ir	20	Mud or adobe	Thatch	10
SC_US	TBD	120	4.8	Conc panels/conc m	BUR/concrete deck	70	Glass curtain	Galv steel/metal bar	20	Stone curtain/conc n	BUR/concrete deck	10
	HD	40	1.6	Conc panels/conc m	BUR/concrete deck	50	Brick veneer/conc m	BUR/wood deck	30	Cement board/wood	BUR/wood deck	20
	LD	8	0.4	Wood frame/wood s	Shingles/wood deck	40	Wood frame/vinyl or	Shingles/wood deck	30	Stone	Ceramic tiles/wood c	30
SE_US	TBD	100	4.0	Conc panels/conc m	BUR/concrete deck	70	Glass curtain	Galv steel/metal bar	20	Stone curtain/conc n	BUR/concrete deck	10
	HD	40	1.6	Conc panels/conc m	BUR/concrete deck	50	Brick veneer/conc m	Galv steel/metal bar	30	EIFS façade/wood fr	Metal tiles	20
	LD	8	0.4	Wood frame/vinyl or	Shingles/wood deck	60	Wood frame/wood s	Shingles/wood deck	20	Stone	Metal tiles	20
SE_Asia	TBD	90	3.6	Conc panels/conc m	BUR/concrete deck	70	Glass curtain	Galv steel/metal bar	30			
	HD	30	1.2	Conc panels/conc m	Ceramic tiles/wood c	80	Brick veneer/conc m	BUR/wood deck	10	Stone curtain/conc n	Galv steel/metal bar	10
	LD	3	0.3	Concrete blocks	Ceramic tiles/wood c	60	Corrugated metal	Corrugated metal (ir	20	Mud or adobe	Shingles/wood deck	20
S_Europe	TBD	120	4.8	Plaster veneer/conc	Ceramic tiles/wood c	70	Brick veneer/conc m	BUR/concrete deck	20	Glass curtain	Galv steel/metal bar	10
	HD	40	1.6	Plaster veneer/brick	Ceramic tiles/wood c	50	Brick veneer/conc m	BUR/concrete deck	30	Plaster veneer/conc	Galv steel/metal bar	20
	LD	8	0.8	Wood frame/stucco	Ceramic tiles/wood c	60	Brick masonry, reinf	Shingles/wood deck	40			
SW_US	TBD	130	5.2	Conc panels/conc m	BUR/concrete deck	70	Glass curtain	EPDM/steel deck	20	Glass curtain	Galv steel/metal bar	10
	HD	40	1.6	Conc panels/conc m	BUR/concrete deck	50	Brick veneer/conc m	Galv steel/metal bar	30	EIFS façade/wood fr	Ceramic tiles/wood c	20
	LD	8	0.4	Wood frame/stucco	Ceramic tiles/wood c	60	Wood frame/vinyl or	Shingles/wood deck	20	Wood frame/wood s	Shingles/wood deck	20
Temp_SA	TBD	120	4.8	Conc panels/conc m	BUR/concrete deck	70	Glass curtain	Galv steel/metal bar	20	Plaster veneer/conc	EPDM/steel deck	10
	HD	40	1.6	Conc panels/conc m	BUR/wood deck	50	Plaster veneer/conc	Corrugated metal (ir	30	Brick masonry, reinf	Ceramic tiles/wood c	20
	LD	8	0.8	Wood frame/wood s	Corrugated metal (ir	50	Mud or adobe	Ceramic tiles/wood c	30	Brick masonry, reinf	Ceramic tiles/wood c	20
Trop_SA	TBD	120	4.8	Conc panels/conc m	BUR/concrete deck	70	Glass curtain	EPDM/steel deck	20	Brick veneer/conc m	Galv steel/metal bar	10
	HD	40	1.6	Conc panels/conc m	BUR/wood deck	50	Concrete blocks	Shingles/wood deck	30	Brick masonry, reinf	Corrugated metal (ir	20
	LD	8	0.8	Wood frame/stucco	Ceramic tiles/wood c	50	Brick masonry, reinf	Corrugated metal (ir	40	Corrugated metal	Corrugated metal (ir	10
W_Africa	TBD	60	2.4	Conc panels/conc m	BUR/concrete deck	80	Glass curtain	EPDM/steel deck	10	Plaster veneer/conc	Galv steel/metal bar	10
	HD	20	0.8	Plaster veneer/brick	Ceramic tiles/wood c	70	Mud or adobe	Corrugated metal (ir	20	Mud or adobe	Ceramic tiles/wood c	10
	LD	3	0.3	Mud or adobe	Mud	50	Concrete blocks	Thatch	30	Wood frame/unins w	Corrugated metal (ir	20
W_Europe	TBD	140	5.6	Conc panels/conc m	BUR/concrete deck	60	Stone curtain/conc n	Ceramic tiles/wood c	20	Glass curtain	Galv steel/metal bar	20
	HD	50	2.0	Brick veneer/conc m	Shingles/wood deck	40	Stone curtain/conc n	Slate tiles	40	EIFS façade/wood fr	Ceramic tiles/wood c	20
	LD	12	1.2	Brick masonry, reinf	Ceramic tiles/wood c	40	Stone	Shingles/wood deck	40	Wood frame/hardbc	Shingles/wood deck	20

Appendix C – Construction material properties

Properties	Thermal Conductivity W/m*K (tk)	Volumetric Heat Capacity J/m^3*K (vc)	Emissivity	Albedo
EXTERIOR/SURFACE MATERIALS				
concrete (cast, dense, reinforced)	1.90	2.10E+06	0.88	0.23
concrete, blocks (hollow, mediumweight)	0.86	7.81E+05	0.94	0.23
painted concrete masonry	n/a	n/a	0.93	0.60
concrete, pre-cast panel	1.28	2.12E+06	0.90	0.23
cement board (cement fiberboard)	0.08	4.55E+05	0.70	0.25
brick (reinforced)	1.10	1.61E+06	0.91	0.3
clay brick (for North America)	0.50	1.52E+06	0.91	0.3
limestone	2.90	2.31E+06	0.86	0.28
granite	3.49	2.42E+06	0.68	0.33
sandstone	1.30	1.81E+06	0.79	0.35
stone average	2.56	2.18E+06	0.78	0.32
mud or adobe	0.60	1.41E+06	0.90	0.35
wood, unpainted	0.14	1.05E+06	0.86	0.40
wood, painted	0.14	1.05E+06	0.84	0.38
siding (aluminum or vinyl)	0.70	2.38E+06	0.91	0.54
hardboard siding	0.12	1.72E+06	0.84	0.49
stucco or plaster	0.60	1.14E+06	0.91	0.65
glass (windows)	1.29	2.19E+06	0.91	0.08
steel	45.00	3.74E+06	0.80	0.18
EIFS base and finish coating	0.59	9.66E+06	0.97	0.69
iron	72.00	4.19E+06	0.21	0.13
tin	65.00	1.75E+06	0.05	n/a
corrugated metal (average iron/tin)	68.50	2.97E+06	0.13	0.17
bitumen (poured asphalt)	1.20	1.93E+06	0.91	0.13
bitumen/felt weighted average	0.95	1.68E+06	0.91	0.13
tile, ceramic	1.20	1.70E+06	0.90	0.23
shingles, asphalt (asphalt roofing)	1.15	1.96E+06	0.91	0.14
shingles/felt weighted average	0.91	1.70E+06	0.91	0.14
EPDM	0.33	2.74E+06	0.87	0.40
slate	1.72	2.31E+06	0.83	0.10
thatch	0.07	4.32E+04	0.91	0.18
zinc	113.00	2.73E+06	0.04	0.61
extruded Polystyrene (XPS)	0.03	4.16E+04	0.91	0.62
expanded Polystyrene (EPS)	0.03	2.90E+04	0.91	0.62
gravel on BUR (roof gravel or slag)	1.44	1.48E+06	0.92	0.35

Appendix C, continued

Properties	Thermal Conductivity W/m*K (tk)	Volumetric Heat Capacity J/m^3*K (vc)
INTERIOR MATERIALS		
drywall (coated gypsum board, exterior)	0.16	6.09E+05
drywall (gypsum board, interior)	0.16	6.09E+05
building paper (sheathing membrane)	0.11	1.64E+06
insulation, wall (glass fiber wool)	0.04	1.01E+04
plywood - roofs	0.15	9.94E+05
sheathing board (plywood) - walls	0.09	9.40E+05
roofing felt (felt sheathing)	0.19	9.12E+05
OSB: oriented strand board	0.09	1.18E+06
timber (softwood)	0.17	1.03E+06
air, still	0.03	1.21E+03
insulation slab/rigid fibrous roof insulation	0.04	9.66E+04
fiber board (asphalt coated)	0.05	6.02E+05
cellular concrete (aerated)	0.70	8.40E+05
rubble	0.80	9.50E+05

Appendix C, continued

Sources for thermal properties

EXTERIOR/SURFACE MATERIALS	
concrete (cast, dense, reinforced)	Clarke 2001
concrete, blocks (hollow, mediumweight)	Clarke 2001
painted concrete masonry	n/a
concrete, precast panel	Clarke 2001
cement board (cement fibreboard)	Clarke 2001
brick (reinforced)	Clarke 2001
clay brick (for North America)	Mukhopadhyaya et al. 2003
limestone	Clarke 2001
granite	Clarke 2001
sandstone	Clarke 2001
stone average	n/a
mud or adobe	Straube and Burnett 2005 and Clarke
wood, unpainted	Clarke 2001 (average of 7 types)
wood, painted	Clarke 2001 (average of 7 types)
siding (aluminum or vinyl)	Mukhopadhyaya et al. 2003
hardboard siding	Mukhopadhyaya et al. 2003
stucco or plaster	Clarke 2001
glass (windows)	Clarke 2001
steel	Clarke 2001
EIFS base and finish coating	Mukhopadhyaya et al. 2003
iron	Clarke 2001
tin	Clarke 2001
corrugated metal (average iron/tin)	n/a
bitumen (poured asphalt)	Clarke 2001
bitumen/felt weighted ave	Weighted average of 1:3 felt to bitumen.
tile, ceramic	Clarke 2001
shingles, asphalt (asphalt roofing)	Clarke 2001
shingles/felt weighted ave	Weighted average of 1:3 felt to shingles
EPDM	Azaar et al 2002
slate	Clarke 2001
thatch	Clarke 2001
zinc	Clarke 2001
extruded Polystyrene (XPS)	Mukhopadhyaya et al. 2003
expanded Polystyrene (EPS)	Mukhopadhyaya et al. 2003
gravel on BUR (roof gravel or slag)	Clarke 2001

Appendix C, continued

Sources for thermal properties

INTERIOR MATERIALS	
drywall (coated gypsum board, exterior)	Mukhopadhyaya et al. 2003
drywall (gypsum board, interior)	Mukhopadhyaya et al. 2003
building paper (sheathing membrane)	Mukhopadhyaya et al. 2003
insulation, wall (glass fiber wool)	Mukhopadhyaya et al. 2003
plywood - roofs	Clarke 2001
sheathing board (plywood) - walls	Mukhopadhyaya et al. 2003
roofing felt (felt sheathing)	Clarke 2001
OSB: oriented strand board	Mukhopadhyaya et al. 2003
timber (softwood)	Mukhopadhyaya et al. 2003
air, still	Straube and Burnett 2005
insulation slab/rigid fibrous roof insulation	Straube and Burnett 2005
fiber board (asphalt coated)	Mukhopadhyaya et al. 2003
cellular concrete (aerated)	Clarke 2001
rubble	Clarke 2001

Appendix C, continued

Sources for emissivity values

EXTERIOR/SURFACE MATERIALS	
concrete (cast, dense, reinforced)	Oke 1987, Clarke, and Omega average
concrete, blocks (hollow, mediumweight)	Clarke and Omega agree
painted concrete masonry	Omega 2007
concrete, precast panel	Clarke 2001
cement board (cement fibreboard)	Infrared Services, Inc. 2007
brick (reinforced)	Oke, Clarke, and Omega average
clay brick (for North America)	Oke, Clarke, and Omega average
limestone	Oke, Clarke, and Omega
granite	Omega and Clarke
sandstone	Omega and Clarke
stone average	average of above three stones
mud or adobe	Omega 2007
wood, unpainted	Clarke and Omega average
wood, painted	Clarke and Omega average
siding (aluminum or vinyl)	Clarke (PVC)
hardboard siding	Clarke and Omega
stucco or plaster	Clarke "plaster"
glass (windows)	Oke, Clarke, and Omega agree
steel	Clarke and Omega agree
EIFS base and finish coating	Fronapfel et al. 2006
iron	Clarke 2001
tin	Omega 2007
corrugated metal (average iron/tin)	Average of iron/tin (above)
bitumen (poured asphalt)	Oke, Clarke, and LBNL agree
bitumen/felt weighted ave	Oke, Clarke, and LBNL agree
tile, ceramic	Oke, Clarke, and LBNL agree
shingles, asphalt (asphalt roofing)	LBNL 2000
shingles/felt weighted ave	LBNL 2000
EPDM	LBNL 2000
slate	Clarke and Omega average
thatch	Schmugge et al. 1988
zinc	LBNL 2000 (galvanized steel)
extruded Polystyrene (XPS)	Clarke 2001
expanded Polystyrene (EPS)	Clarke (PVC)
gravel on BUR (roof gravel or slag)	Oke and Florida Solar Energy Center

Appendix C, continued

Sources for albedo values

EXTERIOR/SURFACE MATERIALS	
concrete (cast, dense, reinforced)	Oke 1987
concrete, blocks (hollow, mediumweight)	Oke 1987
painted concrete masonry	Reagan and Acklam 1979
concrete, precast panel	Oke 1987
cement board (cement fibreboard)	Levinson and Hashem 2001
brick (reinforced)	Oke 1987
clay brick (for North America)	Oke 1987
limestone	Oke 1987
granite	Weast 1981
sandstone	Oke 1987, Levinson and Hashem 2001
stone average	average of three stones above
mud or adobe	Omega 2007 and Oke 1987
wood, unpainted	Wechsler and Glaser 1966
wood, painted	average of Oke, Reagan and Acklam 1979
siding (aluminum or vinyl)	Wechsler and Glaser 1966
hardboard siding	average of Oke, Reagan and Acklam 1979
stucco or plaster	Levinson & Hashem, Reagan & Acklam
glass (windows)	Oke 1987
steel	Akbari and Desjarlais 2007
EIFS base and finish coating	Master Wal, Inc. 2006
iron	Oke 1987
tin	not found
corrugated metal (average iron/tin)	Taha et al. 1992
bitumen (poured asphalt)	Oke, T.R. 1987
bitumen/felt weighted ave	Oke, T.R. 1987
tile, ceramic	Oke 1987, Reagan and Acklam 1979
shingles, asphalt (asphalt roofing)	Berdahl and Bretz 1997
shingles/felt weighted ave	Berdahl and Bretz 1997
EPDM	Taha et al. 1992
slate	Oke 1987
thatch	Oke 1987
zinc	LBNL 2000 (galvanized steel)
extruded Polystyrene (XPS)	Levinson and Hashem 2001
expanded Polystyrene (EPS)	Levinson and Hashem 2001
gravel on BUR (roof gravel or slag)	Reagan and Acklam 1979

Appendix D – Wall and roof assemblies by layer

Wall Type		Layer 1	Layer 2	Layer 3	Layer 4	Layer 5	Layer 6	Layer 7	Layer 8	Layer 9	Layer 10	Total w (m)	Surface	
Conc panels/conc masonry		cncrt pnl	cncrt pnl	air	cncrt blk	cncrt blk	cncrt blk	cncrt blk	XPS	XPS	drywall		precast concrete	
	thickness(m)	0.050	0.039	0.025	0.050	0.050	0.050	0.050	0.013	0.012	0.012	0.351	emissivity	0.90
	tk	1.28	1.28	0.03	0.86	0.86	0.86	0.86	0.03	0.03	0.16		albedo	0.23
	cv	2.12E+06	2.12E+06	1.21E+03	7.81E+05	7.81E+05	7.81E+05	7.81E+05	4.16E+04	4.16E+04	6.09E+05			
Glass curtain		glass	glass	air	air	air	air	air	air	glass	glass		glass	
	thickness(m)	0.004	0.003	0.003	0.002	0.002	0.002	0.002	0.002	0.004	0.003	0.027	emissivity	0.91
	tk	1.29	1.29	0.03	0.03	0.03	0.03	0.03	0.03	1.29	1.29		albedo	0.08
	cv	2.19E+06	2.19E+06	1.21E+03	1.21E+03	1.21E+03	1.21E+03	1.21E+03	1.21E+03	2.19E+06	2.19E+06			
Brick veneer/conc masonry		clay brck	clay brck	air	cncrt blk	cncrt blk	cncrt blk	cncrt blk	XPS	XPS	drywall		brick	
	thickness(m)	0.050	0.039	0.025	0.050	0.050	0.050	0.050	0.013	0.012	0.012	0.351	emissivity	0.91
	tk	0.50	0.50	0.03	0.86	0.86	0.86	0.86	0.03	0.03	0.16		albedo	0.30
	cv	1.52E+06	1.52E+06	1.21E+03	7.81E+05	7.81E+05	7.81E+05	7.81E+05	4.16E+04	4.16E+04	6.09E+05			
Stone curtain/conc masonry		stone	stone	air	cncrt blk	cncrt blk	cncrt blk	cncrt blk	XPS	XPS	drywall		granite, typically	
	thickness(m)	0.015	0.015	0.020	0.050	0.050	0.050	0.050	0.013	0.012	0.012	0.287	emissivity	0.68
	tk	2.56	2.56	0.03	0.86	0.86	0.86	0.86	0.03	0.03	0.16		albedo	0.33
	cv	2.18E+06	2.18E+06	1.21E+03	7.81E+05	7.81E+05	7.81E+05	7.81E+05	4.16E+04	4.16E+04	6.09E+05			
Plaster veneer/brick masonry		plaster	clay brck	air	air	bldg ppr	ext drywll	insulation	insulation	drywall	drywall		plaster	
	thickness(m)	0.013	0.089	0.013	0.012	0.001	0.011	0.050	0.039	0.006	0.006	0.240	emissivity	0.91
	tk	0.60	0.50	0.03	0.03	0.11	0.16	0.04	0.04	0.16	0.16		albedo	0.65
	cv	1.14E+06	1.52E+06	1.21E+03	1.21E+03	1.64E+06	6.09E+05	1.01E+04	1.01E+04	6.09E+05	6.09E+05			
Plaster veneer/conc masonry		plaster	cncrt blk	cncrt blk	cncrt blk	cncrt blk	cncrt blk	cncrt blk	XPS	XPS	drywall		plaster	
	thickness(m)	0.013	0.034	0.034	0.033	0.033	0.033	0.033	0.013	0.012	0.012	0.250	emissivity	0.91
	tk	0.60	0.86	0.86	0.86	0.86	0.86	0.86	0.03	0.03	0.16		albedo	0.65
	cv	1.14E+06	7.81E+05	7.81E+05	7.81E+05	7.81E+05	7.81E+05	7.81E+05	4.16E+04	4.16E+04	6.09E+05			
EIFS façade/wood frame		EIFS	EPS	ext drywll	ext drywll	insulation	insulation	insulation	insulation	drywall	drywall		EIFS tan/gray	
	thickness(m)	0.005	0.038	0.010	0.005	0.020	0.020	0.020	0.029	0.006	0.006	0.159	emissivity	0.97
	tk	0.59	0.03	0.16	0.16	0.04	0.04	0.04	0.04	0.16	0.16		albedo	0.69
	cv	9.66E+06	2.90E+04	6.09E+05	6.09E+05	1.01E+04	1.01E+04	1.01E+04	1.01E+04	6.09E+05	6.09E+05			
Cement board/wood frame		cmnt brd	cmnt brd	air	fiberboard	insulation	insulation	insulation	insulation	drywall	drywall		cement board	
	thickness(m)	0.006	0.006	0.012	0.012	0.020	0.020	0.020	0.029	0.006	0.006	0.137	emissivity	0.70
	tk	0.08	0.08	0.03	0.05	0.04	0.04	0.04	0.04	0.16	0.16		albedo	0.25
	cv	4.55E+05	4.55E+05	1.21E+03	6.02E+05	1.01E+04	1.01E+04	1.01E+04	1.01E+04	6.09E+05	6.09E+05			
Wood frame/hardbrd siding		hb siding	air	OSB	insulation	insulation	insulation	insulation	insulation	drywall	drywall		hardboard siding	
	thickness(m)	0.012	0.001	0.011	0.020	0.020	0.020	0.020	0.009	0.006	0.006	0.125	emissivity	0.84
	tk	0.12	0.03	0.09	0.16	0.04	0.04	0.04	0.04	0.16	0.16		albedo	0.38
	cv	1.72E+06	1.20E+03	1.18E+06	1.06E+06	1.01E+04	1.01E+04	1.01E+04	1.01E+04	6.09E+05	6.09E+05			
Wood frame/wood siding		wood sid	air	plywood	insulation	insulation	insulation	insulation	insulation	drywall	drywall		painted wood	
	thickness(m)	0.012	0.001	0.011	0.020	0.020	0.020	0.020	0.009	0.006	0.006	0.125	emissivity	0.84
	tk	0.14	0.03	0.09	0.04	0.04	0.04	0.04	0.04	0.16	0.16		albedo	0.38
	cv	1.05E+06	1.21E+03	9.40E+05	1.01E+04	1.01E+04	1.01E+04	1.01E+04	1.01E+04	6.09E+05	6.09E+05			

Wall Type		Layer 1	Layer 2	Layer 3	Layer 4	Layer 5	Layer 6	Layer 7	Layer 8	Layer 9	Layer 10	Total w (m)	Surface	
Wood frame/unins wood siding		wood sid	wood sid	wood sid	wood sid	wood sid	air	air	plywood	drywall	drywall		weathered wood	
	thickness(m)	0.004	0.004	0.004	0.002	0.002	0.001	0.001	0.011	0.006	0.006	0.041	emissivity	0.86
	tk	0.14	0.14	0.14	0.14	0.14	0.03	0.03	0.09	0.16	0.16		albedo	0.40
	cv	1.05E+06	1.05E+06	1.05E+06	1.05E+06	1.05E+06	1.21E+03	1.21E+03	9.40E+05	6.09E+05	6.09E+05			
Wood frame/vinyl or Al siding		vnyl siding	air	OSB	insulation	insulation	insulation	insulation	insulation	drywall	drywall		vinyl or Al siding	
	thickness(m)	0.002	0.002	0.011	0.020	0.020	0.020	0.020	0.009	0.006	0.006	0.116	emissivity	0.91
	tk	0.70	0.03	0.09	0.04	0.04	0.04	0.04	0.04	0.16	0.16		albedo	0.54
	cv	2.38E+06	1.21E+03	1.18E+06	1.01E+04	1.01E+04	1.01E+04	1.01E+04	1.01E+04	6.09E+05	6.09E+05			
Wood frame/stucco		stucco	stucco	plywood	insulation	insulation	insulation	insulation	insulation	drywall	drywall		stucco	
	thickness(m)	0.022	0.022	0.011	0.020	0.020	0.020	0.020	0.009	0.006	0.006	0.156	emissivity	0.91
	tk	0.60	0.60	0.09	0.04	0.04	0.04	0.04	0.04	0.16	0.16		albedo	0.65
	cv	1.14E+06	1.14E+06	9.40E+05	1.01E+04	1.01E+04	1.01E+04	1.01E+04	1.01E+04	6.09E+05	6.09E+05			
Brick masonry, reinforced		clay brck	clay brck	air	air	bldg ppr	ext drywll	insulation	insulation	drywall	drywall		brick	
	thickness(m)	0.050	0.050	0.013	0.012	0.001	0.011	0.050	0.039	0.006	0.006	0.238	emissivity	0.91
	tk	1.10	1.10	0.03	0.03	0.11	0.16	0.04	0.04	0.16	0.16		albedo	0.30
	cv	1.61E+06	1.61E+06	1.21E+03	1.21E+03	1.64E+06	6.09E+05	1.01E+04	1.01E+04	6.09E+05	6.09E+05			
Stone		stone	stone	air	air	bldg ppr	ext drywll	insulation	insulation	drywall	drywall		stone (average)	
	thickness(m)	0.100	0.100	0.013	0.012	0.001	0.011	0.050	0.039	0.006	0.006	0.338	emissivity	0.78
	tk	2.56	2.56	0.03	0.03	0.11	0.16	0.04	0.04	0.16	0.16		albedo	0.32
	cv	2.18E+06	2.18E+06	1.21E+03	1.21E+03	1.64E+06	6.09E+05	1.01E+04	1.01E+04	6.09E+05	6.09E+05			
Concrete blocks		conc blk	conc blk	conc blk	conc blk	conc blk	conc blk	conc blk	conc blk	conc blk	conc blk		painted conc msnry	
	thickness(m)	0.020	0.020	0.020	0.020	0.020	0.020	0.020	0.020	0.020	0.020	0.200	emissivity	0.93
	tk	0.86	0.86	0.86	0.86	0.86	0.86	0.86	0.86	0.86	0.86		albedo	0.60
	cv	7.81E+05	7.81E+05	7.81E+05	7.81E+05	7.81E+05	7.81E+05	7.81E+05	7.81E+05	7.81E+05	7.81E+05			
Corrugated metal		metal	metal	metal	metal	metal	metal	metal	metal	metal	metal		iron/tin average	
	thickness(m)	0.001	0.001	0.001	0.001	0.001	0.001	0.001	0.001	0.001	0.001	0.010	emissivity	0.13
	tk	68.50	68.50	68.50	68.50	68.50	68.50	68.50	68.50	68.50	68.50		albedo	0.17
	cv	2.97E+06	2.97E+06	2.97E+06	2.97E+06	2.97E+06	2.97E+06	2.97E+06	2.97E+06	2.97E+06	2.97E+06			
Mud or adobe		mud/adobe	mud/adobe	mud/adobe	mud/adobe	mud/adobe	mud/adobe	mud/adobe	mud/adobe	mud/adobe	mud/adobe		mud or adobe	
	thickness(m)	0.025	0.025	0.025	0.025	0.025	0.025	0.025	0.025	0.025	0.025	0.250	emissivity	0.90
	tk	0.60	0.60	0.60	0.60	0.60	0.60	0.60	0.60	0.60	0.60		albedo	0.35
	cv	1.41E+06	1.41E+06	1.41E+06	1.41E+06	1.41E+06	1.41E+06	1.41E+06	1.41E+06	1.41E+06	1.41E+06			
Rubble		stone	stone	stone	stone	rubble	rubble	stone	stone	stone	stone		stone (average)	
	thickness(m)	0.100	0.100	0.100	0.100	0.050	0.050	0.100	0.100	0.100	0.100	0.900	emissivity	0.78
	tk	2.56	2.56	2.56	2.56	0.80	0.80	2.56	2.56	2.56	2.56		albedo	0.32
	cv	2.18E+06	2.18E+06	2.18E+06	2.18E+06	9.50E+05	9.50E+05	2.18E+06	2.18E+06	2.18E+06	2.18E+06			
Galvanized steel		galv steel	insulation	insulation	insulation	insulation	insulation	air	air	steel	steel		zinc coating	
	thickness(m)	0.003	0.02	0.02	0.02	0.02	0.02	0.004	0.003	0.004	0.004	0.118	emissivity	0.04
	tk	45.00	0.04	0.04	0.04	0.04	0.04	0.03	0.03	45.00	45.00		albedo	0.61
	cv	3.74E+06	1.01E+04	1.01E+04	1.01E+04	1.01E+04	1.01E+04	1.21E+03	1.21E+03	3.74E+06	3.74E+06			

Roof Type		Layer 1	Layer 2	Layer 3	Layer 4	Layer 5	Layer 6	Layer 7	Layer 8	Layer 9	Layer 10	Total w (m)	Surface	
BUR/concrete deck		asphalt	felt	bitumen	ins slab	ins slab	ins slab	ins slab	cllr cncrt	cllr cncrt	cllr cncrt		asphalt	
	thickness(m)	0.007	0.001	0.002	0.040	0.020	0.020	0.020	0.050	0.050	0.050	0.260	emissivity	0.91
	tk	1.20	0.19	1.20	0.04	0.04	0.04	0.04	0.70	0.70	0.70		albedo	0.13
	cv	1.93E+06	9.12E+05	1.93E+06	9.66E+04	9.66E+04	9.66E+04	9.66E+04	8.40E+05	8.40E+05	8.40E+05			
BUR/wood deck		gravel	felt	bitumen	ins slab	ins slab	ins slab	ins slab	tmb/plywd	tmb/plywd	tmb/plywd		gravel/mineral ch	
	thickness(m)	0.007	0.001	0.002	0.030	0.030	0.030	0.030	0.009	0.005	0.005	0.149	emissivity	0.92
	tk	1.44	0.19	1.20	0.04	0.04	0.04	0.04	0.15	0.15	0.15		albedo	0.35
	cv	1.48E+06	9.12E+05	1.93E+06	9.66E+04	9.66E+04	9.66E+04	9.66E+04	9.94E+05	9.94E+05	9.94E+05			
PVC/steel deck		PVC(EPS)	insulation	insulation	insulation	insulation	insulation	air	air	steel deck	steel deck		PVC(EPS)	
	thickness(m)	0.002	0.020	0.020	0.020	0.020	0.020	0.004	0.003	0.004	0.004	0.117	emissivity	0.91
	tk	0.03	0.04	0.04	0.04	0.04	0.04	0.03	0.03	45.00	45.00		albedo	0.62
	cv	2.90E+04	1.01E+04	1.01E+04	1.01E+04	1.01E+04	1.01E+04	1.21E+03	1.21E+03	3.74E+06	3.74E+06			
EPDM/steel deck		EPDM	insulation	insulation	insulation	insulation	insulation	air	air	steel deck	steel deck		EPDM	
	thickness(m)	0.002	0.020	0.020	0.020	0.020	0.020	0.004	0.003	0.004	0.004	0.117	emissivity	0.87
	tk	0.33	0.04	0.04	0.04	0.04	0.04	0.03	0.03	45.00	45.00		albedo	0.40
	cv	2.74E+06	1.01E+04	1.01E+04	1.01E+04	1.01E+04	1.01E+04	1.21E+03	1.21E+03	3.74E+06	3.74E+06			
Galv steel/metal bar joists		galv steel	insulation	insulation	insulation	insulation	insulation	air	air	steel deck	steel deck		zinc coating	
	thickness(m)	0.003	0.020	0.020	0.020	0.020	0.020	0.004	0.003	0.004	0.004	0.118	emissivity	0.04
	tk	45.00	0.04	0.04	0.04	0.04	0.04	0.03	0.03	45.00	45.00		albedo	0.61
	cv	3.74E+06	1.01E+04	1.01E+04	1.01E+04	1.01E+04	1.01E+04	1.21E+03	1.21E+03	3.74E+06	3.74E+06			
Corrugated metal (iron/tin)		metal	metal	metal	metal	metal	metal	metal	metal	metal	metal		iron/tin average	
	thickness(m)	0.001	0.001	0.001	0.001	0.001	0.001	0.001	0.001	0.001	0.001	0.010	emissivity	0.13
	tk	68.50	68.50	68.50	68.50	68.50	68.50	68.50	68.50	68.50	68.50		albedo	0.17
	cv	2.97E+06	2.97E+06	2.97E+06	2.97E+06	2.97E+06	2.97E+06	2.97E+06	2.97E+06	2.97E+06	2.97E+06			
Shingles/wood deck		shingle	felt	plywood	plywood	plywood	plywood	plywood	plywood	plywood	plywood		shingles	
	thickness(m)	0.005	0.001	0.003	0.003	0.003	0.003	0.003	0.003	0.003	0.003	0.030	emissivity	0.91
	tk	1.15	0.19	0.15	0.15	0.15	0.15	0.15	0.15	0.15	0.15		albedo	0.14
	cv	1.96E+06	9.12E+05	9.94E+05	9.94E+05	9.94E+05	9.94E+05	9.94E+05	9.94E+05	9.94E+05	9.94E+05			

Roof Type		Layer 1	Layer 2	Layer 3	Layer 4	Layer 5	Layer 6	Layer 7	Layer 8	Layer 9	Layer 10	Total w (m)	Surface	
Ceramic tiles/wood deck		cer tile	cer tile	cer tile	air	plywood	plywood	plywood	plywood	plywood	plywood		ceramic tiles	
	thickness(m)	0.004	0.003	0.003	0.003	0.004	0.004	0.004	0.004	0.003	0.003	0.035	emissivity	0.90
	tk	1.20	1.20	1.20	0.03	0.15	0.15	0.15	0.15	0.15	0.15		albedo	0.23
	cv	1.70E+06	1.70E+06	1.70E+06	1.21E+03	9.94E+05	9.94E+05	9.94E+05	9.94E+05	9.94E+05	9.94E+05			
Thatch		thatch	thatch	thatch	thatch	thatch	thatch	thatch	thatch	timber	timber		thatch	
	thickness(m)	0.020	0.020	0.020	0.020	0.020	0.020	0.020	0.020	0.010	0.010	0.180	emissivity	0.91
	tk	0.07	0.07	0.07	0.07	0.07	0.07	0.07	0.07	0.17	0.17		albedo	0.18
	cv	4.32E+04	4.32E+04	4.32E+04	4.32E+04	4.32E+04	4.32E+04	4.32E+04	4.32E+04	1.03E+06	1.03E+06			
Slate tiles/wood deck		slate	air	plywood	plywood	plywood	plywood	plywood	plywood	plywood	plywood		slate	
	thickness(m)	0.007	0.003	0.003	0.003	0.003	0.003	0.003	0.003	0.002	0.002	0.032	emissivity	0.83
	tk	1.72	0.03	0.15	0.15	0.15	0.15	0.15	0.15	0.15	0.15		albedo	0.10
	cv	2.31E+06	1.21E+03	9.94E+05	9.94E+05	9.94E+05	9.94E+05	9.94E+05	9.94E+05	9.94E+05	9.94E+05			
Metal tiles/wood deck		galv steel	felt	plywood	plywood	plywood	plywood	plywood	plywood	plywood	plywood		zinc coating	
	thickness(m)	0.001	0.001	0.003	0.003	0.003	0.003	0.003	0.003	0.003	0.003	0.026	emissivity	0.04
	tk	45.00	0.19	0.15	0.15	0.15	0.15	0.15	0.15	0.15	0.15		albedo	0.61
	cv	3.74E+06	9.12E+05	9.94E+05	9.94E+05	9.94E+05	9.94E+05	9.94E+05	9.94E+05	9.94E+05	9.94E+05			
Mud		mud/adobe	mud/adobe	mud/adobe	mud/adobe	mud/adobe	mud/adobe	mud/adobe	mud/adobe	metal	metal		mud or adobe	
	thickness(m)	0.010	0.010	0.010	0.010	0.010	0.010	0.010	0.010	0.002	0.002	0.084	emissivity	0.90
	tk	0.60	0.60	0.60	0.60	0.60	0.60	0.60	0.60	68.50	68.50		albedo	0.35
	cv	1.41E+06	1.41E+06	1.41E+06	1.41E+06	1.41E+06	1.41E+06	1.41E+06	1.41E+06	2.97E+06	2.97E+06			

Appendix D, continued. Descriptions and sources for wall assemblies

Wall Type	Description	Source
Conc panels/conc masonry	Pre-cast concrete panels over reinforced concrete masonry insulated with extruded polystyrene (XPS). Interior is finished with drywall.	Mukhopadhyaya *et al.* 2004b
Glass curtain	Glass wall over steel frame construction. Only glass considered because it has greatest surface area.	Vigener and Brown 2007, Schwartz 2001
Brick veneer/conc masonry	Brick masonry façade over reinforced concrete block masonry insulated with XPS. 25 mm drainage cavity between brick and concrete. Interior is finished with drywall.	Mukhopadhyaya *et al.* 2004b
Stone curtain/conc masonry	Stone façade over reinforced concrete block masonry insulated with XPS. 25 mm drainage cavity between brick and concrete. Interior is finished with drywall.	Scheffler 2007, Mukhopadhyaya *et al.* 2004b
Plaster veneer/brick masonry	Plaster façade over reinforced brick masonry with glass fiber insulation. Interior is finished with drywall.	Mukhopadhyaya *et al.* 2004b, PCA 2007
Plaster veneer/conc masonry	Plaster façade over reinforced concrete block masonry with glass fiber insulation. Interior is finished with drywall.	Mukhopadhyaya *et al.* 2004b, PCA 2007
EIFS façade/wood frame	Exterior Insulation and Finish System (EIFS) (a.k.a. synthetic stucco), insulated with expanded polystyrene (EPS) over wood frame. Interior is finished with drywall.	Mukhopadhyaya *et al.* 2003, 2004a
Cement board/wood frame	Cement board, 12mm air cavity, fiberboard, insulated, installed over wood frame. Interior is finished with drywall.	Maref *et al.* 2007, Mukhopadhyaya *et al.* 2004a
Wood frame/hardbrd siding	Painted hardboard siding installed over oriented strand board (OSB), insulation and wood frame. Interior is finished with drywall.	Mukhopadhyaya *et al.* 2003, Sahal and Lacasse 2004
Wood frame/wood siding	Painted wood siding over plywood, insulation, installed over wood frame. Interior is finished with drywall.	Mukhopadhyaya *et al.* 2003, 2004a
Wood frame/unins wood siding	Uninsulated, unpainted wood plank walls over wood frame. Interior is unfinished, weathered wood.	Mukhopadhyaya *et al.* 2003, 2004a
Wood frame/vinyl or Al siding	Vinyl or aluminum siding installed over OSB, insulation, and wood frame. Interior is finished with drywall.	Mukhopadhyaya *et al.* 2003, 2004a
Wood frame/stucco	Stucco façade over plywood and insulation with wood frame. Interior is finished with drywall.	Mukhopadhyaya *et al.* 2003, 2004a, PCA 2007
Brick masonry, reinforced	Reinforced brick masonry with 25mm air cavity then exterior drywall, insulation. Interior finished with drywall.	Mukhopadhyaya *et al.* 2003, 2004b
Stone	Stone masonry with 25mm air cavity then exterior drywall, insulation. Interior finished with drywall.	Mukhopadhyaya *et al.* 2003
Concrete blocks	Painted, hollow, medium weight concrete block masonry. Interior is likely painted, but otherwise unfinished.	n/a
Corrugated metal	Corrugated metal sheets serve as walls.	n/a
Mud or adobe	Mud or adobe with strengthening medium (e.g. straw, wire mesh). Interior is unfinished.	Binici *et al.* 2005
Rubble	Large stones for interior/exterior wall, cemented with mud or some other simple cementing agent, then infilled with rubble.	Brzev *et al.* 2007
Galvanized steel	Insulated, galavanized steel wall on interior and exterior.	PSBI 2007

Appendix D, continued. Descriptions and sources for roof assemblies

Roof Type	Description	Source
BUR/concrete deck	Built-up-roof (BUR) of asphalt-based materials (e.g. felt, bitumen) over insulated cellular concrete deck.	Foamglas 2005, 2006, Knauf 2005a, BUR thickness: Paroli *et al.* 1996.
BUR/wood deck	Built-up-roof (BUR) of asphalt-based materials over insulated wood deck.	Foamglas 2005, 2006, Knauf 2005a, BUR thickness: Paroli *et al.* 1996.
PVC/steel deck	Polyvinyl chloride (PVC) membrane (typically polyester reinforcing fabric between two PVC sheets) over insulated steel deck.	Knauf 2005a, Baskaran *et al.* 2003
EPDM/steel deck	Ethylene Propylene Diene Monomer (EPDM) single-ply membrane over insulation and steel deck.	Knauf 2005a, Baskaran *et al*. 2003, Roofhelp.com 2007
Galv steel/metal bar	Galvanized steel, insulated, over metal bar joists.	USACE 1998
Corrugated metal	Single layer of corrugated iron or tin.	n/a
Shingles/wood deck	Asphalt shingles over wood deck. Considered to be a cold roof, because insulation is on attic floor or is part of ceiling, not as part of roof.	Knauf 2004b, 2005b
Ceramic tiles/wood deck	Ceramic tiles over wood deck - cold roof, but air pockets provide some insulation.	Knauf 2004b, 2005b
Thatch	Thatch roof supported by timber.	Thatch.org 2007
Slate tiles/wood deck	Slate tiles over wood deck - Considered to be a cold roof, because insulation is on attic floor or is part of ceiling, not as part of roof.	Knauf 2004b, 2005b
Metal tiles/wood deck	Metal tiles over wood deck. Considered to be a cold roof, because insulation is on attic floor or is part of ceiling, not as part of roof.	Knauf 2004b, 2005b
Mud	Mud, usually supported by wire mesh.	Binici *et al.* 2005